Assessing Durability of Cement Kiln Dust Manufactured Aggregates

by

Hun Choi

Submitted in partial fulfilment of the requirements
for the degree of Master of Applied Science

at

Dalhousie University
Halifax, Nova Scotia
March 2018

TABLE OF CONTENTS

LIST OF TABLES

LIST OF FIGURES

ABSTRACT

Accelerated carbonation technology (ACT) is the addition of carbon dioxide and water and/or binder to a waste material to change an initially fine-grained waste material to an aggregate. For use in geotechnical applications, ACT aggregates must be durable. The objective of this thesis is to evaluate the durability (i.e. particle breakage) of a manufactured ACT aggregate made from cement kiln dust (CKD).

For an initial trial of ACT aggregate, several geotechnical tests related to the aggregate's physical and chemical characteristics were performed. After refinement of the manufacturing process, it was shown that much stronger (3 MPa) ACT aggregate from CKD could be achieved. Hardin relative breakage (B_r) was used to compare particle breakage under a variety of loading conditions (triaxial compression, triaxial shear and freeze-thaw) and particle size. It was shown that the 2.5mm to 1.25mm size had superior performance with respect to particle breakage under all the loading conditions.

LIST OF ABBREVIATIONS USED

ACT	Accelerated Carbonation Technology
ASTM	American Society for Testing and Materials
BSI	British Standard Institution
BS EN	British Standard European Norm
B_r	Relative Breakage
CCS	Carbon Capture and Storage
CCU	Carbon capture utilization
CKD	Cement Kiln Dust
C8A	Carbon 8 Aggregate
DEM	Discrete Element Modeling
FA	Fly Ash
F/T	Freeze-Thaw
KPa	Kilopascal
ICP-OES	Inductively Couple Plasma Optical Emission Spectroscopy
LOI	Loss On Ignition
LWA	Lightweight Aggregate
MIP	Mercury Intrusion Porosimetry
MPa	Megapascals
MSWI	Municipal Solid Waste Incineration
RPM	Revolutions per Minute
SEM	Scanning Electron Microscopy
TGA	Thermogravimetric Analysis
W/S	Water/Solid Ratio
XRF	X-Ray Fluorescence
XRD	X-Ray Diffraction

ACKNOWLEDGEMENTS

Thanks to my supervisor Dr. Craig Lake and external supervisor Dr. Colin Hills for all their help and support. I have been extremely lucky to have a supervisor who cared so much about me and my work, and who responded to my questions and queries so promptly.

I also want to mention assistance from the graduate coordinator Dr. Hany El Naggar and lab technicians Blair Dickins, Brian Kennedy and Jesse Keane. I would also like to thank the Civil and Resource Engineering staff; Shelley Parker, June Ferguson and Lynn Peters.

Thank you to Wenwen, Meagon, Reza, Sara, Marshi and Jaman, my office friends for willingness to lend a helping hand. Completing this work would have been even more difficult were it not for the support and friendship provided by the other members of the office friends, family and the member of the Department.

Finally, I would like to thank again my supervisor Dr. Craig Lake, not only for providing the funding which allowed me to undertake this research, but also for giving me a great help and advice for me as a supervisor and mentor.

Chapter 1. Introduction

1.1 General

International requirements for construction aggregates (i.e. roadways, concrete, asphalt, etc.) is ever increasing. Through 2017, global consumption of aggregates is forecast to expand by 5.8% to 53.2 billion metric tons (Freedonia Group, 2013). Unfortunately, in many geographical areas, aggregate supply is limited; meanwhile in developed countries, environmental permitting of mineral workings is becoming increasingly difficult. Sustainable aggregate manufacturing is one potential solution to these challenges.

Accelerated carbonation technology (ACT) utilizes fine mineral and waste materials in the production of engineering products, including lightweight and relatively low strength aggregates (Gunning *et al*., 2009). The process is patented and commercially used in the UK to produce aggregate from industrial waste for use in concrete block manufacturing (CIWM, 2014). In essence, ACT involves a chemical reaction with calcium-based minerals in the waste and carbon dioxide (CO_2). The reaction products can cause rapid hardening of the calcium minerals and cementation between grains to form agglomerations or monolithic materials. Carbonation can occur naturally by the reaction between alkaline materials and atmospheric CO_2. However, this natural reaction is very slow due to the low concentration in the atmosphere. ACT uses a higher concentration of CO_2 to complete this same reaction within hours (Costa *et al*. 2007; Huijgen & Comans, 2005a). Water is added to form a thin aqueous film around the particles of the material. The water layer reacts with the calcium phases in the material

to form calcium hydroxide and water. Carbon dioxide injected into the mixture then reacts with the aqueous film forming carbonic acid. Calcium ions from the calcium hydroxide react with carbonate ions of the carbonic acid to form calcium carbonate. The process is performed with a pelleting process such that aggregates are formed with concentric layers of carbonate with a "hard outer shell". The carbonation process is exothermic, releasing heat as well as free water (Fernández *et al*. 2004a; Arandigoyen *et al*, 2006; Domingo *et al*., 2006).

Cement kiln dust (CKD) is a significant by-product material of the cement manufacturing process. It is an alkali-rich waste derived from cement manufacture, which is normally sent to landfills if not used for other beneficial reuse products. The past decade has seen significant changes in the management of CKD, thus reducing the amount disposed to landfill (Adaska & Taubert, 2008). In the USA, approximately 1Mt of CKD is produced every year (14 kg for every tonne of cement clinker), with 85% of this being landfilled (PCA, 2011). The US cement industry has agreed to reduce the amount of CKD landfilled by 60% while also curbing carbon dioxide emissions by 10% compared with 1990 levels (PCA, 2011). Among the largest cement producers, there is an overall drive towards resource and energy efficiency through the Cement Sustainability Initiative (CSI, 2016). Therefore, technologies that can make use of the gaseous and solid wastes from cement manufacture can potentially make a valuable contribution to achieving these goals. In this respect, accelerated carbonation has been demonstrated as a commercially viable means of recycling calcium-rich solid waste streams (such as CKD) as new construction products while permanently sequestering carbon dioxide (Carbon8, 2016).

CKD offers significant potential for the manufacturing of sustainable aggregates using Accelerated Carbonation Technology (ACT) due to a high calcium oxide (CaO) content and the potential to develop stronger, more durable aggregate than that currently being developed from other industrial wastes. An additional advantage is the sequestration of carbon dioxide into a waste stream, resulting in a process that has a carbon dioxide footprint ('carbon footprint') much lower than sintered, kiln-fired or quarried and transported natural stone (see Table 1).

Table 1. Categories and examples of light weight aggregate (LWA) (modified from BS EN 13055:2016 (BSI, 2016: Table A.2)

Source material	LWA type
Natural LWA	Pumice, scoria, tuff
Manufactured LWA from natural source materials	Expanded clay, expanded shale, expanded slate, expanded perlite, expanded vermiculite
Manufactured LWA from by-products or recycled source materials	Sintered fly ash, cold-bonded fly ash, foamed blast-furnace slag, expanded blast-furnace slag, expanded glass, foamed glass
LWA as by-products of industrial processes	Furnace clinker, furnace bottom ash, fly ash

1.2 Thesis Aims and Objectives

This thesis presents the results of a laboratory study that evaluates the geotechnical and geo-environmental properties of a manufactured aggregate derived from cement kiln dust (CKD) and produced using a lab-scale version of the ACT process. This process operates at commercial scale in the UK, producing aggregates from many different

types thermal residual. In this study the ACT process relies on the accelerated reaction of carbon dioxide with the calcium oxide in the CKD material in the presence of water. No additional binder was used in this study, relying solely instead on the formation of carbonate to form the aggregate.

The objectives of this thesis are to:

1) Provide a literature review related to topics in this thesis (i.e. ACT process, CKD, aggregate durability, etc.)
2) Perform the ACT process in Dalhousie laboratories and assess the physical and chemical properties of the resulting aggregates developed from the CKD material studied.
3) Assess the durability of the resulting aggregate under different loading conditions (i.e. physical durability) and freeze-thaw (F/W) (i.e. environmental durability) using commonly employed durability assessment techniques. A further objective is to assess the role of particle size on the observed durability of the manufactured aggregate studied in this thesis.

To carry out these objectives, the thesis has been organized into the following chapters:
Chapter 2: This chapter provides a literature review related to the science behind carbonation and various high levels issues related to carbonation and its applications. Literature related to the ACT process is reviewed as well as factors that can affect the aggregates produced. Given that CKD is the study waste in this thesis, a brief review of CKD is also provided in this chapter.
Chapter 3: In this chapter, the aggregate manufacturing process for the CKD derived aggregate is briefly described. To explore future potential construction applications of

the aggregate, several geotechnical test results are used to assess strength and durability (i.e. individual particle strength, internal shear strength of the particle assemblage, wet–dry testing, freeze–thaw testing). Screening tests on the aggregate's geo-environmental characteristics are discussed (metal leaching, dissolved heavy metal adsorption and hydraulic conductivity) to assess potential uses further.

Chapter 4: This chapter examines in further detail the durability of the CKD aggregate described in Chapter 3 with particular focus on geotechnical applications. Particle breakage is used as a measure to assess the ACT aggregate durability under physical and environmental (i.e. freeze-thaw) loadings. The role of particle size of the ACT aggregate is also explored with respect to understanding the causes of particle breakage in the study.

Chapter 5: This chapter provides a summary of the work in the thesis and provide recommendations for future research.

Chapter 2. Literature Review

2.1 Carbonation

Natural carbonation is a slow process, taking years or decades, due to the low concentration of carbon dioxide in the atmosphere (Van Ginneken *et al.*, 2004). The carbonation process can be accelerated by exposing the reactive material (cement, lime or reactive waste) to an elevated concentration of carbon dioxide (Johnson *et al.*, 2003; Liu *et al.*, 2001; Maries *et al.*, 2001). The accelerated carbonation process can completed within several hours or even minutes (Roy *et al.*, 1999).

2.2 General Chemistry of the Mineral Carbonation Process

Mineral carbonation is a naturally occurring weathering process where alkaline earth metals (Ca, Mg) combine with carbon dioxide to form stable carbonates. Even though the reactions are highly exothermic, they occur slowly in nature during the gradual physiochemical weathering of silicate minerals, such as serpentine ($Mg_3Si_2O_5(OH)_4$), olivine (Mg_2SiO_4) or wollastonite ($CaSiO_3$) (Meylan, Moreau & Erkman, 2015):

$$Mg_3Si_2O_5(OH)_2\ (s) + 3CO_2\ (g) \rightarrow 3MgCO_3(s) + 2H_2O + 2SiO_2\ (s)$$

$$Mg_2SiO_4\ (s) + 2CO_2\ (g) \rightarrow 2MgCO_3\ (s) + SiO_2\ (s)$$

$$CaSiO_3\ (s) + CO_2\ (g) \rightarrow CaCO_3\ (s) + SiO_2\ (s)$$

When CO_2 reacts with metal oxides (indicated here as MO, where M is a divalent metal, e.g., calcium and magnesium) the corresponding carbonate is formed and heat is released according to the following chemical reaction:

$MO + CO_2 \rightarrow MCO_3 + heat$

Minerals containing substantial quantities of Mg and Ca-oxide undergo carbonation in the presence of CO_2. The basic reactions can be given for the Mg and Ca oxides as (Huntzinger *et al*., 2009):

$CaO + CO_2 \rightarrow CaCO_3 + 179$ KJ/mol

$MgO + CO_2 \rightarrow MgCO_3 + 118$ KJ/mol

Pure calcium and magnesium oxides are rare in nature, however, many minerals containing a chemical combination of these oxides can be found in nature in abundant quantities.

2.3 Accelerated Carbonation Process

The technology of accelerated carbonation is used in the waste management industry to accelerate the natural carbonation process. It uses high purity CO_2 to penetrate into solid wastes by diffusion of CO_2 to make the reaction much faster than diffusion by atmospheric CO_2, and the reaction can be finalized within a few minutes or hours (Costa *et al*., 2007; Fernández *et al*., 2004b).

In the process of accelerated carbonation, carbon dioxide gas is introduced into a mixture of alkaline materials, in presence of water. The following process takes place:

• A thin aqueous film is formed around the particles of the alkaline materials

• Water reacts with calcium oxide (CaO) phases of the alkaline material to form calcium hydroxide ($Ca(OH)_2$)

$$CaO + H_2O \Rightarrow Ca(OH)_2$$

• Carbon dioxide from surrounding atmosphere gets absorbed into the aqueous film forming carbonic acid (H_2CO_3)

$$CO_2 + H_2O \Rightarrow H_2CO_3$$

• The calcium hydroxide ($Ca(OH)_2$) and carbonic acid (H_2CO_3) combine to form calcium carbonate ($CaCO_3$):

$$H_2CO_3 + Ca(OH)_2 \Rightarrow CaCO_3 + H_2O$$

The carbonation is exothermic, releasing significant heat as well as free water (Fernández *et al*. 2004a).

Using accelerated carbonation technology, carbon capture storage (CCS) and carbon capture utilization (CCU) aim to reduce CO_2 emissions and reuse thermal waste materials from point sources such as power plants and industrial processes (Bleys, 2016). The difference between CCS and CCU is in the final destination of the captured CO_2. In CCS, captured CO_2 is transferred to a suitable site for long-term storage (Markewitz *et al*, 2012; Edward *et al*, 2015; Zapp *et al*, 2012). While in CCU, captured CO_2 is converted into commercial products and a permanent mineral (Markewitz *et al*, 2012; Styring *et al*, 2011; Bleys, 2016).

One of the advantages of CCU over CCS is that utilization of CO_2 is normally a profitable activity as products can be sold (Styring *et al*., 2011). Furthermore, compared to conventional petrochemicals feed stocks, CO_2 has the advantage of being a 'renewable' resource (as long it continues to be emitted by various industrial activities); low in cost and non-toxic.

2.4 Applications

2.4.1 Carbon Capture

Power plants, oil refineries, biogas sweetening as well as production of ammonia, ethylene oxide, cement and iron and steel are the main industrial sources of CO_2 (Markewitz *et al*, 2012; Edward *et al*, 2015; Styring *et al*, 2011). For example, over 40% of the worldwide CO_2 emissions are caused by electricity generation in fossil-fuel power plants. Therefore, these sources are the main candidates for a potential application of CCS or CCU. As for the CO_2 capture, a one-size-fit-all technology would not be feasible owing to the diversity of the industrial processes generating CO_2 emissions (Alberta Government, 2015; Edward *et al*, 2015). For that reason, there is a wide variety of CO_2 capturing systems, to ensure compatibility with the specific industry (Bleys, 2016).

2.4.2 CO_2 Storage Options

Once captured, CO_2 is compressed and shipped or pipelined to be stored either in the ground, ocean or as a mineral carbonate (SCOT, 2015; Cooper & Phillips, 2009; Li *et al*, 2013). One option, known as geological storage, involves injecting CO_2 into geological formations such as depleted oil and gas reservoirs, deep saline aquifers and coal bed formations, at depths between 800 and 1000 m (Edward *et al*, 2015; Cooper & Phillips, 2009). Mineral carbonation ‘mineral sequestration’ can be considered as both storage and utilization option. The latter applies if the intended application of the carbonates goes beyond storing CO_2 to be used as a material (Assen *et al*, 2013; SCOT, 2015).

2.4.3 CO_2 Utilization Options

2.4.3.1 Industrial Waste Utilization Using Carbonation

The simplest approach to mineral carbonation would be to react gaseous CO_2 with a metal-oxide bearing phase. Unfortunately, such direct gas-solid reactions are too slow to be practical. Moreover, it is likely to require a higher pressure, temperature and/or suitable pretreatment (Lackner *et al*., 1997).

One of the ways to lower the cost of carbonation process is the use of alkaline industrial waste (Huijgen *et al*., 2005b; SCOT, 2015; Uibu & Kuusik, 2009) specifically fly and bottom ash, concrete waste and slag, residues from municipal waste combustion or steel production. Waste commonly occurs in a pulverized form and thus does not require additional mechanical processing. Calcium and/or magnesium oxides are usually unbounded and their release to the solution is much faster than that of natural minerals (Bauer *et al*., 2011; SCOT, 2015; SETIS, 2016). The industrial waste does not have to be mined and, moreover, a relevant installation can be placed close to a waste source, thus lowering the overall cost. Additionally, hazardous waste can be deactivated through pH-neutralization and mineral transformation. On the other hand, the storage capacity of industrial waste is limited and dependent on developments of technology (Mun & Cho, 2013; Sanna *et al*., 2014; Uibu & Kuusik, 2009). Possibilities of using domestic fly ashes have also been examined (Uliasz-Bochenczyk, 2011; Uliasz-Bochenczyk *et al*., 2012). The studies presented so far has led to a clear conclusion that industrial residues have a potential for quick CO_2 binding with acceptable yield under ambient conditions (Sanna *et al*., 2014).

2.4.3.2 Commercial Application of Accelerated Carbonation

Accelerated Carbonation Technology (ACT) was first developed by researchers working at the University of Greenwich. Research into the use of ACT in the treatment of municipal solid waste extends back to 2002. In 2006 the spin-out company Carbon8 Systems Ltd. was formed to commercialize the processes for waste treatment applications (University of Greenwich, 2012).

A second independent company, Carbon8 Aggregates was founded in May 2010 to utilize Carbon8's technology. The first UK plant was built at Brandon in Suffolk to process Air Pollution Control residue (APCr) from Grundon Waste Management (GWM) energy from a waste plant at Colnbrook, near Heathrow, UK. The plant supplied manufactured carbonated aggregate to an independent masonry block maker, Lignacite from 2012 (University of Greenwich, 2012). Lignacite later developed the Carbon Buster building block, which is said to be the first carbon-negative masonry block in the world. A second line was added to the Brandon plant (also to treat APCr from Colnbrook) in 2014. The second UK facility based at Avonmouth near Bristol (a £5m project) became operational in February 2016. Currently Carbon8 Aggregates are manufacturing 150-200 kt aggregate per year, with production expected to rise to 500 kt/yr by 2021, as another 3 to 4 UK plants come on stream.

2.5 ACT Aggregate Production Variables

2.5.1 Water/Solid (W/S) Ratio and Humidity

Moisture is a key controlling factor to manufacture ACT aggregates, as it affects carbon

dioxide hydration and the carbonation reaction (Rendek, Ducom & Germain, 2006). The optimum moisture content of this manufacture can be affected by the material properties such as the moisture content of the raw materials, particle size distribution and surface area. (Johnson *et al*., 2003).

It has been shown that carbonation slows down substantially in a saturated material due to reduced diffusion, and proceeds when the pores have dried sufficiently to allow CO_2 ingress (Cultrone *et al*., 2005; Russell *et al*., 2001). In addition, when pores are saturated, only the exterior shell of the materials are carbonated (Venhuis & Reardon, 2003). A 50~65% moisture content range is very effective for the carbonation reaction (Russell *et al*., 2001).

Calcium carbonate surfaces are less hydrophilic than the calcium hydroxide they replace, expelling water from the reacted zone (Beruto *et al*., 2005). A complicating factor is that the carbonation reaction is exothermic; which may result in pore water evaporating and causing premature drying of the material before the carbonation reaction reaches completion (Young *et al*., 1974).

2.5.2 Porosity, Grain Size & Surface Area

The diffusion of carbon dioxide is controlled by the pathways into the material (e.g. cracks or pores, and the reaction surface available). High porosity materials are associated with a higher rate and extent of carbonation (Khunthongkeaw *et al*., 2006). The reaction is also promoted by the presence of a large reaction surface (Arandigoyen *et al*., 2006). However, in very fine-grained materials with large surface areas, the

reaction is inhibited due to tighter particle packing, restricting carbon dioxide permeation (Zhang *et al*., 2004). Similarly, low porosity materials will readily suffer from pore blocking as reaction products precipitate in the pore space (Johnson *et al*., 2003). Conversely, fine grained materials may benefit from improved binder dispersion, increased particle contact, and improved cementation due to closer packing (Barnard *et al*., 2005; Molenaar & Venmans, 1993; Huang & Airey, 1998). The ideal material for carbonation will exhibit a small particle size, high porosity and a large surface area (Cultrone *et al*., 2005; O'Connor *et al*., 2005; Khan & Lynsdale, 2002).

2.5.3 Pelleting Rotation Speed

According to Gunning (2011), ACT agglomerates can become enlarged by increasing the speed of the drum. Conversely, reducing the drum speed was found to limit aggregate growth. Gunning (2011) reported that at 10rpm, the mean pellet size was 4.2mm and at 50rpm, the mean size was 13.5mm. It was also noted that the rotation speed also affected pellet strength. At 10rpm, mean pellet strength was between 0.04 and 0.08MPa; at 40 rpm the dry strength increased to 0.18MPa; and at a rotation speed of 50rpm the dry strength of the aggregates fell to 0.13MPa (Gunning, 2011).

2.6 Cement Kiln Dust

Cement Kiln Dust (i.e. CKD) is composed of fine particulates of unburned and partially burned raw materials from the cement production process and is collected from the combustion gases within the pre-heater and kiln systems (Gunturi, *et al*., 2014; Hossain, 2011; Jain & Goliya, 2014). CKD accounts for 15-20% of the cement clinker production (Upma & Kumar 2015).

CKD is gray to tan in color and relatively uniform in size. The particle size distribution of CKD depends on the process technology, method of dust collection, chemical composition of CKD and alkali content. Table 2 lists some typical physical properties of CKD (Rafat, 2006).

Table 2. Typical CKD physical properties (Rafat, 2006)

Property	Value
Gradation (75% passing)	0.03mm (no. 450 sieve)
Maximum particle size	0.3mm(no. 50 sieve)
Specific surface (cm^2/g)	4600 – 14000
Specific gravity	2.6 – 2.8

CKD is derived from the same raw materials as Portland clinker and despite that it has similar chemical composition to Portland cement, significant variation in physical and chemical composition of CKDs can be obtained from different cement plants. Compounds of lime, iron, silica and alumina constitute the major chemical composition of CKD (Rafat, 2006). Table 3 gives the typical chemical composition for CKD and investigated by several researchers. CKDs on the average are typically characterized by higher alkali and sulfur content which is one of the main reasons for removing the dust from kilns. The pH of CKD water mixtures is generally more than 12, and is considered caustic (Gunturi, *et al*., 2014)

Table 3. Typical chemical properties (Kent & Bhavna, 2016)

Parameter (%)	Cement Kiln Dust (CKD)			
	Maslehuddin *et al* (2008)	Sreekrishnavilasam *et al* (2006)	El-aleem *et al* (2005)	Al-Harthy *et al* (2003)
CaO	49.3	43.99	42.99	63.80
SiO_2	17.1	15.05	13.37	15.80
Al_2O_3	4.24	6.75	3.36	3.60
MgO	1.14	1.64	1.90	1.90
Na_2O	3.84	0.69	3.32	0.30
K_2O	2.18	4.00	3.32	3.00
Fe_2O_3	2.89	2.23	2.29	2.80
SO_3	3.56	6.02	5.10	1.70
LOI	15.8	21.6	16.0	-

In many cement plants, nearly half of the CKD can potentially be returned to the kiln system for the manufacture of clinker. Cement kiln dust has the potential for reuse in many different applications included the stabilization/solidification of waste materials, agricultural soil amendment, and stabilization/consolidation of soils. Because of the wide variation in the chemical and physical composition of the landfilled CKD, CKD removed from existing landfills for any beneficial use would be a site-specific decision.

2.7 Research Gaps

This chapter has shown that significant literature exists related to the science behind carbonation and the engineering process of accelerated carbonation (i.e. factors in the process that influence the size and physical and chemical properties of the aggregates). A brief review of cement kiln dust (CKD) has also been presented to provide the reader

with some general knowledge of the material.

Given the relative “newness” of the ACT aggregate production process, little was found in the literature related to aggregate durability. It will be shown in Chapter 4 that significant literature exists for evaluating natural aggregates for durability properties but few, if any, detailed studies have focused on the durability of ACT aggregates for geotechnical applications. The chapters that follow will further explore the issue of the durability of a CKD ACT aggregate by first producing the aggregate, evaluating its physical and chemical properties, and finally undertaking some durability assessments that simulate typical geotechnical loadings expected in field conditions.

Chapter 3. Development of an ACT Aggregate from Cement Kiln Dust (CKD)

3.1 Introduction

The purpose of this chapter is to introduce the physical and chemical characteristics of the CKD material used to produce the ACT aggregates. In addition, the pelletising methods used for the aggregates are described. Resulting physical and chemical properties of the aggregates are then evaluated with via common geotechnical test methods. Preliminary assessment of the physical durability of the aggregates are also evaluated under mechanical and environmental loading conditions.

3.2 Materials

3.2.1 Cement Kiln Dust

The CKD utilized in this research was sampled from a Lafarge cement plant in Brookfield (Nova Scotia, Canada) in August 2014. Two randomly selected samples of the CKD (i.e. CKD-1 and CKD-2) were submitted to SGS Mineral Services Geochemical (Lakefield, Ontario, Canada) for x-ray fluorescence (XRF). XRF sample preparation used a borate fusion method in which an oxidized sample was dissolved in molten flux at temperatures of around 1000 ºC. XRF analysis was conducted on the fused beads.

As with the XRF analysis, two random samples of the CKD (i.e. CKD-3 and CKD-4) were submitted to Dalhousie University's Mineral Engineering Research Centre for elemental analysis. Sample preparation involved oven-drying the samples at 60ºC for

24hr, and then grinding using a mortar and pestle to less than 40 μm. Approximately 2.5g of the sample was then mixed with 5ml of nitric acid (HNO_3), 5ml of hydrofluoric acid (HF) and 2 ml of chloric acid ($HClO_3$), and heated for 12 hours by gradually raising the initial temperature of 25ºC to a final temperature of 205ºC. When finished, 5ml of hydrochloric acid (HCl) was added to digest the sample for 15 minutes at 120ºC followed by the addition of 15ml of deionized water for 15 minutes at 120ºC. The digested sample was then diluted and elements analysed by inductively coupled plasma optical emission spectrometry (ICP-OES) using a Varian CCD simultaneous ICP-OES device.

Tables 4 and 5 show the results of the XRF and elemental analyses for the CKD. The majority of the CKD consists of calcium, iron, silica, aluminum, magnesium and potassium oxides. Of particular note is the 42% CaO content. The high loss on ignition (LOI) for this sample indicates that the CKD has relatively low amounts of reactive free lime (Bhatty *et al*. 1996; Asha & Maria 2006; Mackie *et al*. 2010). The approximately 10 percent of oxides unaccounted for are likely sulfur oxides, (not measured by the method employed) as suggested by results in Table 3.

The detection limits of ICP-OES Instruments are provided in appendix A for reference.

Table 4. Major oxide results for the CKD used in this study

Oxide	CKD-1: %	CKD-2: %
Calcium oxide (CaO)	42·2	42.3
Silicon dioxide (SiO_2)	13·1	12.9
Potassium oxide (K_2O)	5.5	5.5
Aluminium oxide (Al_2O_3)	3.8	3.8
Iron (III) oxide (Fe_2O_3)	1.3	1.3
Magnesium oxide (MgO)	1.1	1.1
Sodium oxide (Na_2O)	0.3	0.3
Titanium dioxide (TiO_2)	0.2	0.2
Phosphorus pentoxide (P_2O_5)	0.03	0.3
Manganese oxide (MnO)	0.04	0.05
Chromium (III) oxide (Cr_2O_3)	0.01	0.01
Vanadium (V) oxide (V_2O_5)	<0.01	<0.01
LOI	22.4	22.2
Sum	90.0	89.7

Table 5. Elemental analysis for the CKD used in this study [a]

Metal	Concentration: mg/kg		Metal	Concentration: mg/kg	
	CKD-3	CKD-4		CKD-3	CKD-4
Silver (Ag)	0.8	0.7	Lithium (Li)	42	42
Aluminium (Al)	20470	20800	Magnesium (Mg)	6614	6750
Barium (Ba)	315	310	Manganese (Mn)	329	326
Beryllium (Be)	0.6	0.6	Sodium (Na)	2499	2554
Calcium	283579	280539	Nickel (Ni)	15	13
Cerium (Ce)	13	13	Phosphorus (P)	149	150
Cobalt (Co)	5	5	Lead (Pb)	158	156
Chromium (Cr)	10	9	Sulfur (S)	43643	43619
Copper (Cu)	13	11	Strontium (Sr)	355	359
Iron (Fe)	9275	9058	Titanium (Ti)	1046	1063
Potassium (K)	48887	49380	Vanadium (V)	39	39
Lanthanum (La)	10	10	Zinc (Zn)	19	19
			Zirconium (Zr)	27	27

[a] Arsenic (As), bismuth (Bi), cadmium (Cd), gallium (Ga), indium (In), molybdenum (Mo), niobium (Nb), antimony (Sb), selenium (Se), tin (Sn) and tantalum (Ta) were below detection limits of the instrument

3.3 Pelletising Process Used to Produce the ACT Aggregates

The moisture content, premixing time and rotation speed can all affect the size and/or strength of the aggregate produced during the ACT process (Russell *et al*. 2001; Beruto *et al*. 2005; Gunning, 2011). In this research, ACT aggregate particle size was controlled by premixing time and water content. Table 6 shows the proportions of CKD and water used in the mixing process (based on previous trial and error by the authors). Batching of aggregates consisted of premixing 400g (dry mass) of CKD with 130g water using a laboratory paddle mixer. During this phase of the mixing process, CKD with water mixed for 90 seconds (60 seconds at 50 rpm speed mixing and 30 seconds at 120 rpm speed mixing). Subsequently, an additional 60g of CKD was added to the mixer and mixed for an additional 90 seconds at 50 rpm to produce more rounded aggregates. The mix was then placed in a rotating drum for 20 minutes at 50 rpm drum to make the aggregate (based on work reported by Gunning, 2011). Figure 1 shows a photograph of the aggregate produced by this ACT process.

Unless otherwise noted, the ACT aggregates in this study were cured under laboratory temperature (20 ± 2°C) and relative humidity (~25%) conditions for at least 28 d prior to being subjected to any testing. This air curing is representative of the likely field curing conditions that would occur (i.e. in a silo). Figure 2 shows the resulting grain size distribution of three subsamples taken from the ACT aggregate produced from the pelleting process described earlier. As shown in Figure 2, and quantified in Table 6, there was very little variability in the aggregate grain size distribution produced using this process. The poorly graded sand, as determined from ASTM D2487 (2011c), had relative density and moisture absorption properties as reported in Table 7.

Table 6. ACT-derived CKD aggregate mix design and pelleting production process

CKD: g	Water: g	Premixing: s	Pelleting time in drum: min	Drum rotation speed: rpm
460	130, 60 at 50 rpm	30 at 120 rpm, 90 at 50 rpm	20	50

rpm, revolutions per minute

Figure 1. ACT-derived CKD aggregate (photograph by author)

Table 7. Grain size, relative density and absorption of ACT derived CKD aggregates

Sub-sample	D_{10} (mm)	D_{30} (mm)	D_{60} (mm)	C_u	C_c	Group Classif-ication	Density(SS) [a]	Absorp-tion (%)
1	1.4	2.0	3.3	2.4	0.9	SP	2.1	25.4
2	1.4	2.0	3.3	2.4	0.9	SP	2.1	25.4
2	1.4	2.1	3.3	2.4	0.9	SP	2.1	25.4

[a] Determined from ASTM D2487 (2011c), SSD, saturated surface dry; SP, poorly graded sand

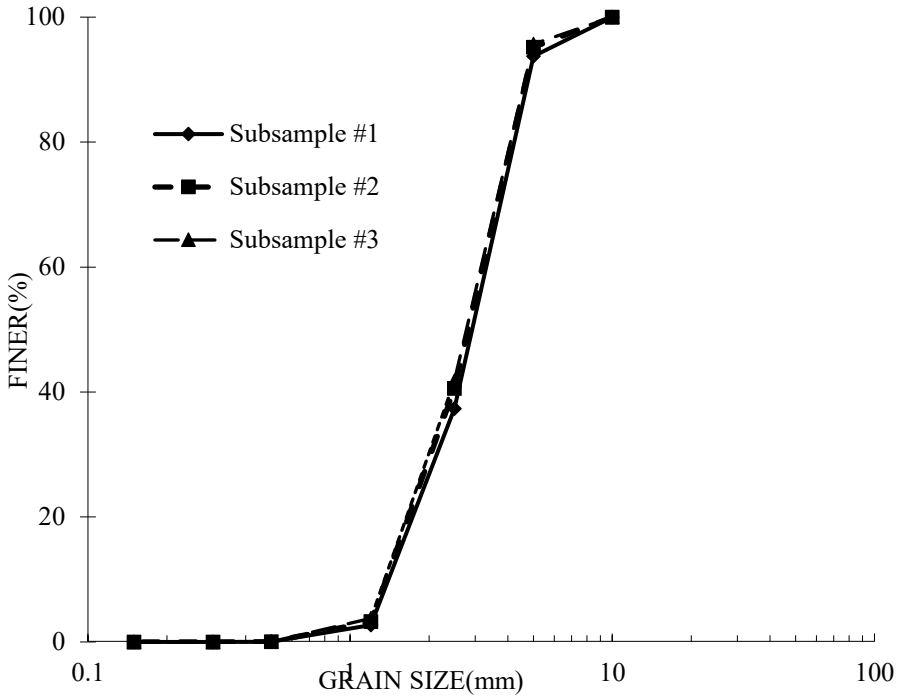

Figure 2. Grain size distribution of ACT aggregate

3.4 ACT Characterization: Aggregate Testing

The ACT aggregate produced from the pelleting process was subjected to a variety of physical and chemical testing to evaluate basic properties. The sections that follow describe these various tests.

3.4.1 Internal Porosity via Mercury Porosimetry

Various factors such as porosity, pore size distribution and absorption can influence the durability properties of an aggregate (Richardson 2009; Mindess *et al*. 2003). The ability of the pores in the aggregate to redistribute moisture during freeze/thaw or wet/dry events relate to many factors, but internal pore size distribution plays an

important role. As discussed by Richardson (2009), aggregates with pore sizes ranging from 0.1 μm to 10 μm seem prone to freeze-thaw problems, as water distributed in these pore sizes have difficulty escaping during freezing events. Conversely, for large pores (i.e. greater than 1 μm as discussed by Richardson 2009), water has the ability to leave the aggregate during freezing events and hence are less likely to be damaged.

To assess the internal pore size of the ACT aggregate, mercury intrusion porosimetry (MIP) was used. Simms and Yanful (2004) reviewed the concepts of MIP testing for examining the internal pore sizes of soils. MIP involves forcing mercury into the pores of a moisture-free material under increasing amounts of pressure. The pressure required to push the mercury (a non-wetting fluid) into cylindrically shaped pores of diameter d is given by the Washburn equation (Washburn, 1921):

$$P = \frac{4\mathrm{TsCOS}\theta}{\mathrm{d}} \qquad (1)$$

where P is the absolute pressure, T_s is the surface tension and θ is the contact angle between the mercury and the soil. Prior to testing, the samples were dried at a temperature of 150°C for at least 24 h to remove fluid from the pores. Several aggregate particles were weighed and placed in the sample holder prior to placement in the porosimeter (Poremaster 60, Quantachrome, USA). The sample cell was then filled with mercury, the pressure in the sample cell was increased incrementally and the volume of mercury intruded into the pores was recorded. Equation 1 was used in combination with these measurements by the Poremaster software to develop a relationship between intruded pore volumes and pore diameter for the ACT aggregate.

3.4.2 Strength

3.4.2.1 Individual Particle Strength

A single pellet compressive strength test is specified in ASTM D4179-11 (2011a) for use with formed catalyst shapes and this method was modified for single aggregate particles. The pellet strength was calculated using equation (2) as described by Arslan & Baykal (2006) and Li *et al*. (2000). Each aggregate diameter was measured at three different axes by Vernier caliper. The single pellet strength was then measured using Wykeham Farrance loading frame and proving ring (see Figure 3). The reported aggregate strength was calculated from the mean value of at least 10 aggregate particles. Aggregates were tested at 7 days, 14 days and 28 days of air curing.

Figure 3. Individual particle strength apparatus

$$S = 2.8Pc/\pi D^2 \quad (2)$$

where

S: the aggregate computed compressive strength (MPa)

Pc : the failure load (MN)

D: the aggregate diameter (m)

3.4.2.2 Particle Assemblage Shear Resistance via Drained Triaxial Testing

Any application in which an aggregate will be subjected to shear stresses (i.e. roadways, drainage on slopes etc.) will require knowledge of the drained internal angle of friction ϕ' of the material. To estimate ϕ', consolidated isotropic drained (CID) triaxial testing was performed on the ACT aggregate assemblage under a relatively loose compaction state (i.e. a conservative approach) to establish its shear resistance under confining stress. To meet the ASTM D7181 (2011b) requirements for particle size, the material described in Figure 2 was passed through a 4·75-mm sieve prior to testing. Sample preparation involved placing a sample membrane on the split mould and filling the mould and membrane partially with de-aired water. The ACT aggregates were then placed in equally spaced layers in the split mould, by allowing the aggregate to free fall through the water. After the placement of a layer of ACT aggregate, light tamping of the aggregate was performed ten times in a circular pattern by using a wooden rod (49 g, 3-cm end diameter) dropped from a height of 5 cm. This was repeated for each of the six layers such that the total compaction energy was 1·3 KJ/m3. The final specimen diameter was 70mm and the height was 150mm. Triaxial testing used an effective confining pressure of 35 kPa followed by a saturation stage (ASTM D7181, 2011b).

After saturation was completed, the drainage lines were opened and the samples were then consolidated under the desired effective confining pressure (i.e. 100, 150, 200 or 250 kPa). Consolidation was deemed to be complete when the sample volume change, as measured using an S-500 triaxial/permeability panel manufactured by Durham GeoSlope indicator (USA), ceased. Axial loading of the sample then began at a strain-controlled rate of 2mm/min. This strain rate met the ASTM D7181 (2011b) requirements for drainage during shear. Failure of the sample was either taken as the maximum value of the major principal stress σ_1 or at 15% axial strain if the maximum value was not reached. Axial displacement of the specimen during testing was measured with a linear variable differential transformer (LVDT) (0.01–10.00mm range; MPE, UK), while axial load on the sample was measured with a 1-kg capacity load cell. LVDT and load cell measurements were recorded using a data acquisition system and software (GDS Instruments, UK). After completion of the triaxial test, the specimen was air-dried and the physical appearance of the aggregate was visually observed. Failure stresses from triaxial tests were plotted in p'–q' space. The definition of p' and q' are as previously described by Lambe & Whitman (1969):

$$p' = \frac{\sigma'_1 f + 2\sigma'_3 f}{3} \quad (3)$$

$$q' = \sigma'_1 f - \sigma'_3 f \quad (4)$$

Where:

$\sigma'_1 f$ = maximum effective major principal stress at failure

$\sigma'_3 f$ = maximum effective minor principal stress at failure

$\sigma'_1 f$ - $\sigma'_3 f$ = deviator stress at failure

3.4.3 Durability

3.4.3.1 Particle Breakage Evaluation

Natural carbonate sands have shown a propensity to be susceptible to particle breakage under high compression stresses (Altuhafi & Coop, 2011). A similar behavior may be anticipated by the carbonated aggregates studied in this research.

Researchers have used various types of tests to evaluate the particle breakage of aggregate assemblages (Lee & Farhoomand, 1967; Valsangkar & Holm, 1999), but testing usually involves some form of compression or shear test on the sample and monitoring changes in particle size before and after, testing. In this research, the change in the grain size of the ACT aggregate after isotropic compression in a triaxial cell was used to evaluate particle breakage (see Lee & Farhoomand, 1967). Although not a standard method, it has been used by other researchers (e.g. Hardin, 1985) to demonstrate particle breakage of aggregates. Similar to the triaxial testing sample preparation mentioned previously, the material shown in Figure 2 was passed through a 4·75-mm sieve prior to testing, compacted in a split mould and subjected to saturation under an effective confining pressure of 35 kPa. The sample was then subjected to consolidation under an effective confining pressure of 300 kPa (a mid-range stress level that would represent a typical upper bound stress for construction applications). The grain size curves of the aggregate were compared before and after the triaxial consolidation to assess any particle breakage that might have occurred.

3.4.3.2 Wet/Dry Cycling

The slake durability test is useful in determining the durability of rocks or weak aggregate under wetting and drying conditions (ASTM D 4644-08, 2008). The testing involved placing a known dry weight of the ACT aggregates (400g) into the drum of the apparatus shown in Figure 4. The drum consists of a mesh with a nominal aperture size of 2.3 mm, with a length of 100 mm and a diameter of 140 mm. The drum was then rotated with the water level approximately 20 mm below the drum axis. The drum was rotated at a speed of 10 rpm for a period of 10 minutes.

After slaking for 10 minutes, aggregates were then dried in an oven at a temperature of 105°C for up to 6 hrs. The mass of dried samples was weighed to obtain the mass remaining after the first cycle. The test was repeated for another cycle and the dry mass again reported. The percent of sample remaining after these wet-dry cycling tests was then recorded.

Figure 4. Wet/dry cycle test apparatus

3.4.3.4 Freeze Thaw

As noted by Edwards (2006), it is important to understand any changes in aggregates as they undergo freeze–thaw. Disintegration of aggregates to a finer grain size after freeze–thaw could cause unwanted settlement or instability in roadway applications or clogging in drainage applications. Past studies have shown that resistance to freeze thaw cycling can be influenced by the aggregate moisture content and strength (Edwards, 2006). In this study, the initial aggregate grain size (400g sample) as shown in Figure 2 was initially soaked in water for 4 h. After soaking, the aggregates were allowed to surface dry for approximately 15 min. The test aggregate samples were then subjected to 10 or 20 freeze–thaw cycles that included freezing to −17·5 ± 2·5°C for 24 h and then thawing in a water bath at room temperature (~20 ± 2°C) for 4 h (see BSI, 2016). The temperatures chosen reflect the British standard BS EN 130055-1:2002 (BSI, 2016). After the end of the freeze–thaw cycles, the samples were subjected to grain size analysis to compare particle size distributions before and after the freeze–thaw cycling. In addition, MIP testing as described in section 3.5.1 was performed on the aggregate before and after freeze–thaw to examine the potential for changes in pore size distribution after freeze–thaw.

3.4.4 ACT Aggregate Geo-environmental Properties: Single Point Heavy Metal Ion Batch Testing

CKD is normally landfilled due to its high pH, particle size and soluble heavy metals. Thus, the potential for the ACT aggregate to be used in practice will ultimately rely on the management of risk, including leaching of any contaminants (i.e. metals) from the

aggregate. To assess metals leaching, a modification of the British standard for evaluating wastes was used (BSI, 2002). The procedure involved taking a 20-g sample of the aggregate (not crushed to reflect actual conditions) and combining it with 200 g of deionized water in glass bottles. The bottles were then rotated for 24 h, after which the resultant leachate was filtered through a 0·45-mm filter. The samples were then subjected to metal analyses with ICP-OES by using a Varian CCD simultaneous ICP-OES device. If the aggregate were to be used in any type of permeable barrier application for metal retention (i.e. storm water, acid drainage, wastewater etc.), knowledge of the capacity of the aggregate to sorb metals is required. To establish estimates of sorption properties of the ACT aggregate for potential metal removal applications, a modified version of ASTM C 1733 -10 was used (ASTM C 1733-10, 2010). Since the goal of the testing was to examine quickly the sorption properties for a range of different metal solutions, the modification involved a single-point batch sorption test which was adopted with separate 500 mg/l solutions of chromium, zinc, cadmium, arsenic, lead and copper, combined with 10 g (dry weight) of the ACT aggregates. Each 200 ml solution and ACT aggregate was placed on a rotating shaker table for 48 h at 100 rpm. After 48 h, the samples were vacuum filtered through a fritted-glass crucible fitted with filter paper to retain the precipitate. After filtering, two to three drops of nitric acid were added to each of the filtered solutions and the samples were then submitted to Dalhousie University Clean Water Laboratory Centre for analysis. Each metal was quantified by ICP mass spectrometry analysis. The potential to use the aggregate for drainage in roadway applications, septic system drainage, permeable reactive barriers and so on requires an estimate of the hydraulic conductivity. The hydraulic conductivity of the aggregate was established by way of the constant head

test method (ASTM D 2434-68, 2006). Hydraulic conductivity tests used ACT-derived CKD aggregates air-cured for 7 d. The samples were loosely tamped into constant head permeameters by using an approximate energy level of 7900 J/m^3.

3.5 Aggregate Test Results

3.5.1 Internal Porosity via Mercury Porosimetry

Figure 5 shows the pore size distribution of the CKD aggregate, as measured by MIP. It can be seen that the majority of pores ranged from approximately 0·01 mm to slightly less than 1 mm. As noted by Richardson (2009), this pore size distribution may be an indication of freeze–thaw susceptibility, although other factors such as particle size, particle strength, pore length, mineralogy, absorption and specific gravity can also have an influence. Also shown in Figure 5 is the pore size distribution of the aggregate after 20 cycles of freeze–thaw. It appears that there was very little change in the pore structure of the aggregate after 20 cycles of freeze–thaw. Rupturing of the pores due to freeze–thaw damage would not be detected by this test method, as this would result in particle breakage of the aggregate. Hence, any major changes in pore size that could cause rupture would be detected only visually or through changes in grain size; this is discussed further in the section 3.4.3.3.

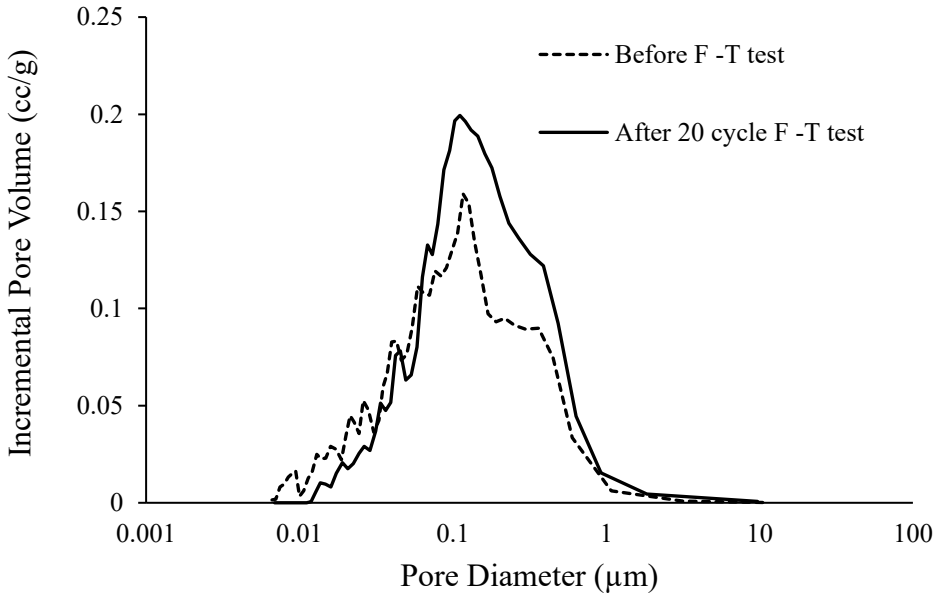

Figure 5. Pore diameter of the ACT as measured by MIP (before and after 20 cycles of freeze–thaw)

3.5.2 Strength

3.5.2.1 Individual Particle Strength

As shown in Figure 6, average individual aggregate strengths reached 0.8 MPa after 7 days of curing, 1.1 MPa after 14 days of curing and 1.2 MPa after 28 days of curing. This strength gain is due to carbonation/hydration continuing over 28 days. Aggregate strengths are rarely measured for construction applications as usually the unconfined compressive strengths of the parent rock would be known. It should be noted that the strengths reported in Figure 6 are comparable to commercially available sintered light-weight aggregates (e.g. Lytag sintered aggregate strength: 0.4 MPa; see Gunning, 2011).

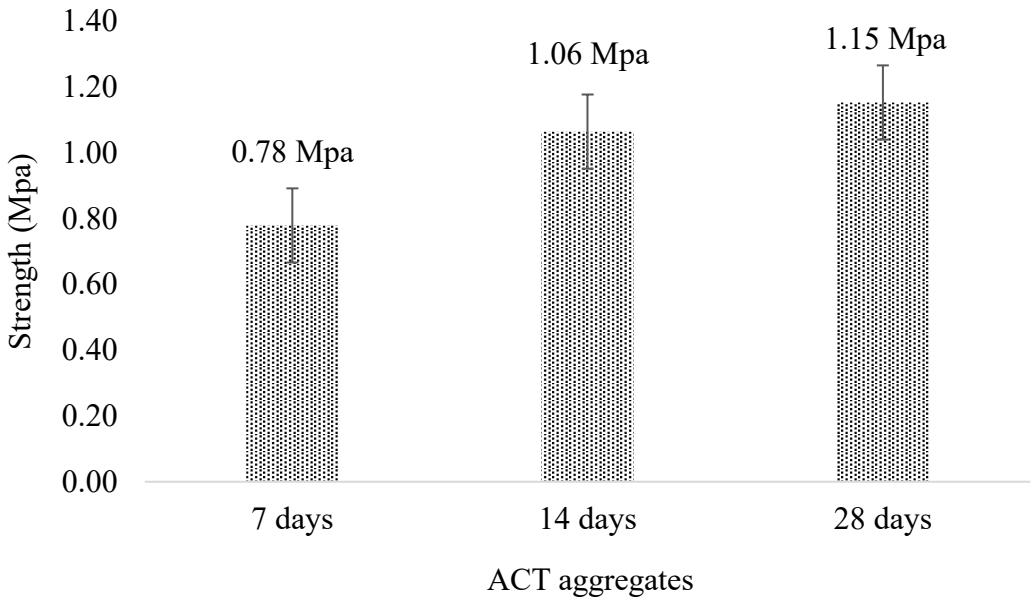

Figure 6. Average ACT individual aggregate strength related to curing time (error bars denote 1 standard deviation from the mean)

3.5.2.2 Particle Assemblage Shear Resistance via Drained Triaxial Testing

Isotropic drained triaxial test results are shown on Figure 7. As would be expected for a moderately compacted soil (dry unit weights for the ACT samples tested ranged from 11.5 kN/m3 to 11.7 kN/m3), deviator stresses at failure exhibited little, if any, peak value with slow sustained increases to the maximum axial stress. The failure stresses, when plotted in p'-q' space (Figure 8) show a linear trend of failure as the confining pressures increased. When fitting a regression line through the origin, the drained friction angle of the aggregate is established as 39°. It is interesting to note that the shear strength envelope remains linear at the higher confining pressures which suggests that there is no significant grinding or crushing of the aggregate resulting in a degradation of strength. No particle breakage was observed in post-test inspection of the aggregate.

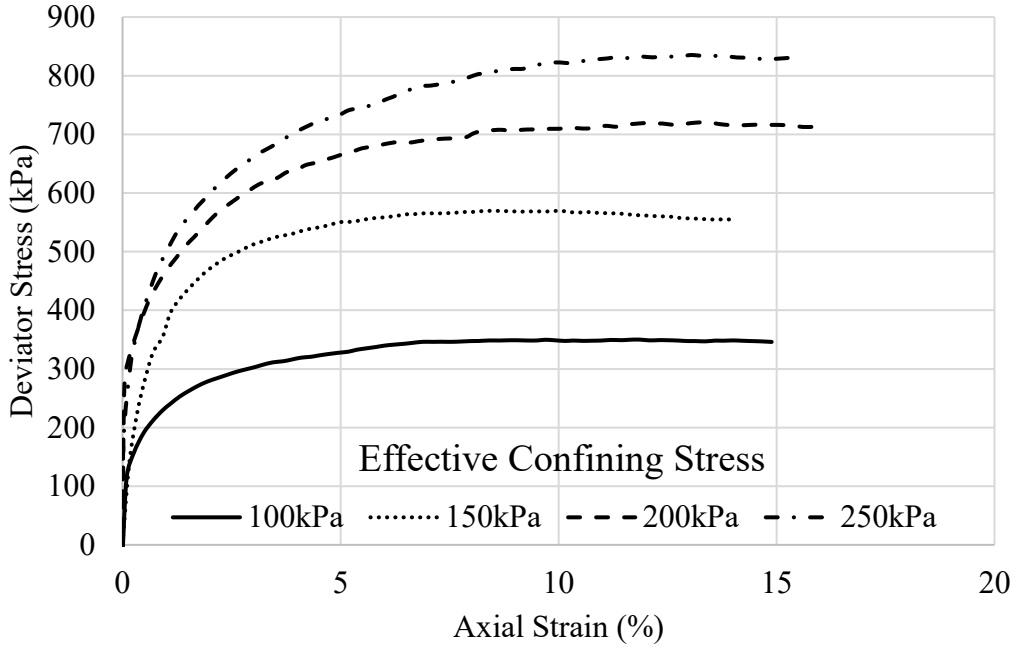

Figure 7. Stress–strain curves for triaxial testing

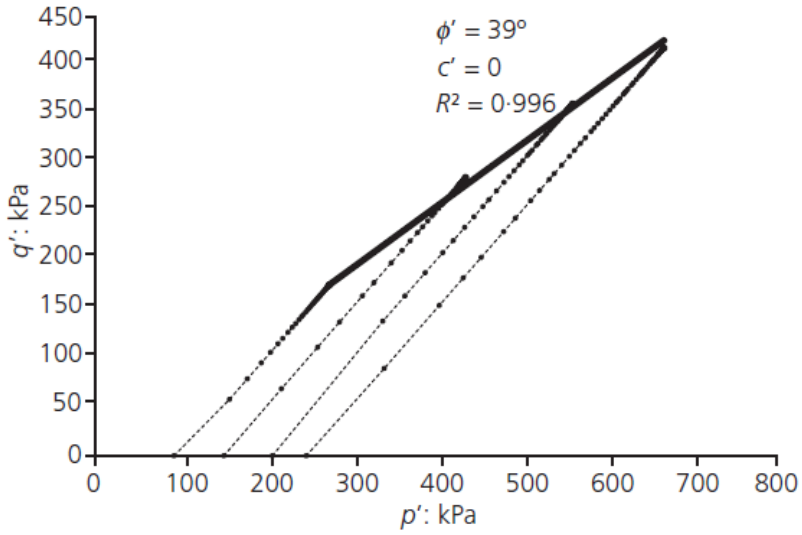

Figure 8. Failure envelope for ACT aggregate from CKD triaxial testing

3.5.3 Durability

3.5.3.1 Particle Breakage Evaluation

The particle size distributions for the ACT aggregate before and after isotropic consolidation in the triaxial cell at 300 kPa are shown in Figure 9. As can be seen from the figure, very little, if any, changes in the grain size of the sample occurred after the application of the 300 kPa effective stress on the sample. No visual deterioration of the test, resulted in very little change in the ACT aggregate after two cycles. Although this is a fairly empirical test method designed for rock materials, according to the Gamble (1971) classification, the aggregate achieved a very high durability rating.

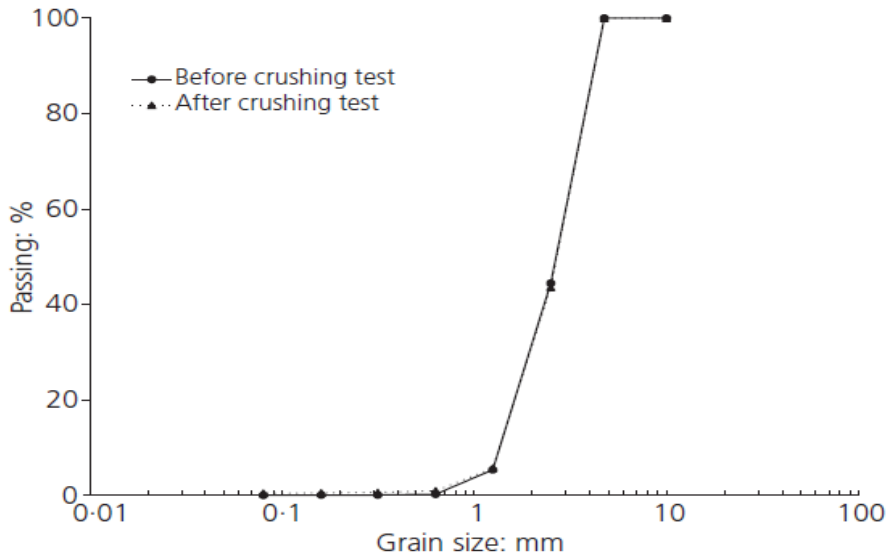

Figure 9. Comparison of grain size curves before and after triaxial consolidation at an effective confining pressure of 300 kPa

3.5.3.2 Wet/Dry Strength Test

The results of the slake durability test is presented in Table 8. The wet-dry cycling as performed using the slake durability test resulted in very little change in the ACT

aggregate after 2 cycles. Although this is a fairly empirical test method designed for rock materials, according to the Gamble (1971) classification, the aggregate achieved a very high durability rating.

Table 8. Slake durability test results

Before test: g	After first cycle: g	After second cycle: g	Slake durability index, I_d: %	Slake durability classification (Gamble, 1971)
400	397·2	395·3	98·8	Very high durability

3.5.3.3 Freeze/Thaw Cycle Tests

As discussed in the section 3.4.3.3, two subsamples of aggregates were subjected to 10 or 20 freeze–thaw cycles. Grain size distributions before and after the freeze–thaw cycling are shown in Figure 10. The grain size distribution before freeze–thaw is presented in comparison with the range of grain size observed in Figure 2 (error bars in Figure 10). Unlike the two previous durability tests, freeze–thaw cycling appeared to have an effect on the grain size of the aggregate. After ten cycles of freeze–thaw, the 2·5-mm aggregate fractions became noticeably finer, while less change at this fraction was observed at the end of the 20^{th} freeze–thaw cycle. Overall, there was a general shift in the original grain size distribution curve, moving to a finer grain size. Photographs of the ACT aggregate during the freeze–thaw cycling process are provided in Figure 11 and show an apparent reduction in the size of the larger aggregates, as opposed to that of the smaller aggregates. The breakage of the 5-mm particles appeared to result from the flaking of the outer surface of the aggregate.

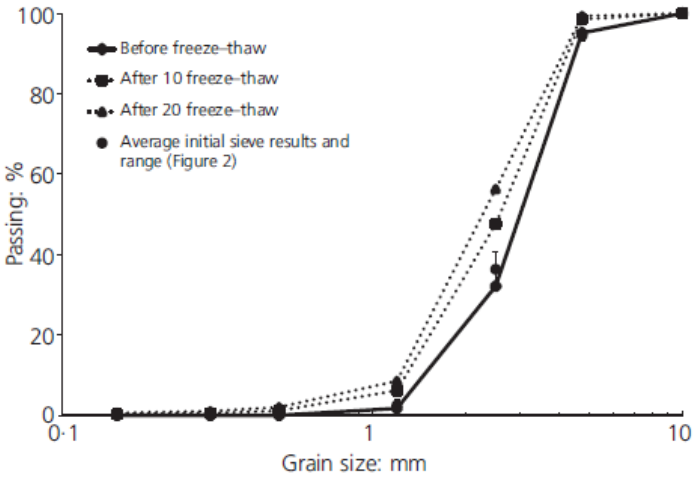

Figure 10. Results of freeze–thaw cycling; comparing grain size distributions before and after 10 and 20 cycles of freeze–thaw

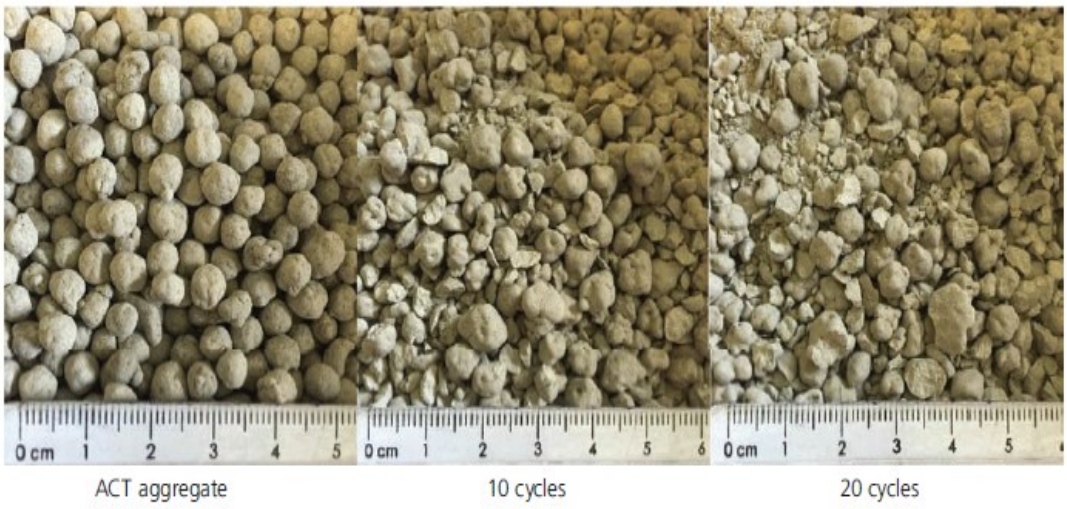

Figure 11. ACT aggregate before and after 10 and 20 cycles of freeze–thaw

3.5.4 ACT Aggregate Geo-environmental Properties: Single Point Heavy Metal Ion Batch Testing

The leaching test results for the ACT aggregate are shown in Table 9. The table shows the results of triplicate analyses of the aggregate (ACT-1, ACT-2, ACT-3) compared with the average total mass of the metals reported in the CKD sample in Table 5. Results are reported in terms of both mass of metal leached per dry mass of ACT (to allow

comparison with Table 5) and leachate concentrations. Only the metals detected in Table 5 are reported in Table 9. As can be seen from Table 9, of the metals detected in the ACT aggregate from Table 5, many did not leach from the aggregate to any appreciable level; many were below the detection limit of the method. Also shown in Table 9 for comparison with leachate values are groundwater standards that must be met in the province of Nova Scotia (NSE, 2014), Canada (the source of the CKD), for remediation. Barium, chromium, strontium and zinc leaching was observed for the aggregate, but at levels below the groundwater guidelines provided in Table 9. As noted from the results in Table 9, there was minimal leaching of the metals shown from the ACT aggregate and the table provides an insight into the ability of the carbonation process to stabilize and solidify CKD.

The single-point batch tests with the heavy metal ions and the ACT aggregate allowed for a preliminary assessment of the aggregate's adsorptive properties for potential reactive barrier applications. As noted in Table 10, very good removal rates were observed for all of the heavy metals tested. The pH in the flasks ranged from 11·3 to 11·5 after 48 h of mixing with the ACT aggregate and metal solutions. The alkaline nature of the ACT aggregate likely contributed to the high removal rates as well as the high absorption ability of the aggregate (i.e. internal porosity).

Table 9. Leaching test results on ACT aggregate

Metal	Leached mass per mass of ACT aggregate: mg/kg			Percentage of average values of Table 3: %	Average leachate concentrations: mg/l	Nova Scotia provincial guidelines, environmental quality standards for groundwater (NSE, 2014) : mg/l
	ACT-1	ACT-2	ACT-3			
Aluminium	12.9	15.6	23.6	0.1	1736	-
Barium	0.5	0.5	1.0	0.2	66	1000
Chromium	0.1	0.1	0.1	1.0	12	25
Copper	0.2	0.3	0.6	3.0	34	-
Strontium	11.8	11.6	12.6	3.4	1205	4400
Zinc	0.2	0.3	0.6	2.0	38	5000

a Silver, arsenic, beryllium, cadmium, cobalt, manganese, nickel, lead, antimony, selenium, tin, titanium, thallium (Tl) and vanadium were below detection limits of the instrument

Table 10. Single-point heavy metal ion batch testing

Heavy metal ion	Concentration of heavy metal ions: mg/l		Removal rate: %
	Initial concentration	Final concentration	
Chromium	507.4	38.8	92.4
Zinc	546.8	52.0	90.5
Cadmium	534.6	1.3	99.8
Arsenic	511.8	20.2	96.0
Lead	480.2	4.6	99.0
Copper	450.2	27.7	93.8

3.6 Discussion

The use of waste to generate new construction materials that are fit for purpose offers significant sustainability gains. A ‘cold’ process, such as used here, will have low energy requirements and result in an attractive carbon footprint. Other benefits include (a) a route for the valorisation of waste that would otherwise be disposed of in landfill, (b) a feedstock that can substitute for virgin stone and (c) carbon dioxide, otherwise released to the atmosphere, is permanently sequestered into the aggregate as a carbonate cement. The objective of this work was to explore the carbonation potential of CKD to produce an aggregate that has physical and chemical properties that enable beneficial reuse in, for example, concrete, roadway engineering, drainage materials or reactive permeable barriers. One of the attractive properties resulting from cementation by carbonation is the low density compared with that of most natural aggregates (bulk density of 1100 kg/m^3 compared with >2000 kg/ m^3, respectively). As aggregates produced in the geosphere are normally formed at great depth and at elevated temperature, they tend to be dense in nature. However, when using ACT to carbonate waste at or near normal atmospheric temperatures and pressures, the density of the carbonate-cemented product is technically ‘lightweight’, although not as lightweight as some sintered or bloated commercially manufactured aggregates (see Table 11 for a comparison). Thus, the CKD-based aggregate is lighter than natural aggregate, but denser (both particle and bulk) than expanded clay, shale and glass aggregates and sintered fly ash. The manufactured aggregates listed in Table 9 (with the exception of the C8A aggregate) are produced using very energy intensive processes, primarily extreme heating, and have high carbon footprints.

The individual particle strength of the CKD aggregate is within the range of those of the other aggregates shown in Table 11. In comparison with the particle strengths of the Nova Scotian quarried aggregate, which range from 25 to 300 MPa, the particle strength of carbonated CKD aggregate is low, and its freeze–thaw resistance, particle breakage (under wet–dry), compression and shear conditions are, not surprisingly, inferior. However, it would be suitable as a fill material for roadway construction given its adequate performance in wet–dry testing and triaxial compression and shear. In the province of Nova Scotia, the use of 'borrow' material for fill is limited little by specification (see NSTIR (2014)) and more by its engineering performance properties and environmental characteristics (NSE, 2014) in determining that an aggregate is 'fit for purpose' in roadway construction applications. Given its good drainage and lightweight characteristics, the aggregate would be beneficial as backfill for retaining structures. The low bulk density relative to those of natural aggregates and the adequate internal angle of friction would serve to reduce loads on the retaining wall, resulting in more economical designs (i.e. smaller walls). Further applications such as in permeable reactive barriers where the sorption of metals is important could be another application for investigation. For the specific metals examined here, over 90% were removed from the solution in single-point sorption tests on exposure to the CKD aggregate. Removal of the metals is likely due to the internal porosity available within the aggregate as well as the alkaline aggregate surface, which promotes metal precipitation; as such, the potential interaction of the aggregate and the groundwater passing through a permeable barrier would have to be assessed using long-term testing/modelling studies.

Table 11. Comparison of physical properties of various manufactured aggregates

	Lecas[a]	Lytag[b]	C8A[c]	Poraver[d]	Solite[e]	This study
Description	Lightweight expanded clay	Sintered fly ash	Carbonation-stabilised waste	Expanded glass	Expanded shale	ACT aggregate from CKD
Bulk density: kg/m^3	215–285	750	950–1100	190–400	720–880	1200 (from hydraulic conductivity)
Dry particle density	0·4–0·6	1·45	1·94	0·3–0·9	Not specified	2·1 (SSD)
Water absorption: % by Weight	28	17·5	18·8	14–35	Not specified	25·4
Individual particle strength: MPa	0·89[f]	3·86[f]	3·13[f]	3·13[f] Not specified	Not specified	1·15[f]

[a] Weber Saint-Gobain (2016), [b] Lytag (2016), [c] Carbon8 (2016), [d] Poraver (2016),
[e] Nesolite (2016), [f] Evaluated as part of this study by using the methods described in 'Individual particle strength' section, C8A, Carbon8 Aggregate

3.7 Summary and Conclusions

To assess the geotechnical and geo-environmental properties of carbonated aggregate made from CKD, several performance tests were applied to gauge potential reuse options. The sand product was shown to have a mature individual aggregate strength of more than 1 MPa and, upon compaction, a friction angle of 39° when subjected to drain triaxial testing under confining pressures ranging from 100 to 250 kPa. The aggregate displayed a very high durability to wet–dry cycling using the slake durability test and no noticeable changes in grain size when subjected to an isotropic confining compression test. Freeze–thaw cycling at −17·5 ± 2·5°C for 20 cycles showed a reduction in grain size that warrants further investigation and future improvement. One-point batch adsorption showed that the ACT aggregate removed 90% of the selected heavy metals from prepared solutions, indicating potential for geo-environmental applications such as permeable reactive barriers.

The resulting grain size and hydraulic conductivity of the aggregate suggest that it is a reasonably permeable material that may be used in drainage or permeable reactive barrier applications.

Based on the results of this chapter, it is apparent that durability of the aggregate under geotechnical loading conditions will be key to addressing its use in geotechnical practice. Hence the focus of Chapter 4 will be the durability of the CKD derived aggregate under various loading scenarios. The emphasis of this work will be the role of particle size and gradation on particle breakage. Given this is a manufactured aggregate and particle sizes can be modified slightly by changing the manufacturing process, if an optimal particle size and/or gradation can be found that will improve particle breakage, this will be beneficial.

Chapter 4. Assessing the Influence of Particle Size on Particle Breakage of ACT Aggregates under Physical and Environmental Loadings

4.1 Introduction

The durability of coarse grained soil particles in geotechnical applications has been the subject of numerous studies in the literature due to concerns related to particle breakage (i.e. large dams) (Marsal, 1967), deep foundations (Klotz & Coop, 2001), roadways (Zheghal, 2009), railway ballast (Indraratna *et al*., 2005), and petroleum applications (Zheng & Tannant, 2016). Particle breakage will result in smaller particles being generated from larger particles which can lead to soil compression under load as well as a potential reduction in soil strength. Work by Marsal (1967); Lee & Farhoomand (1967); Hardin (1985) represent examples of early studies performed to investigate the durability of soil particles by examining particle breakage.

It has been shown in these studies, and others, that the amount of soil particle breakage will depend, inter alia, on the individual soil particle's mineralogy, shape, and size. Coop and his research team have examined natural uncemented carbonate sand (i.e. calcareous sand) previously (Coop 1990) and have shown the susceptibility of these soils to compression and particle breakage under various stress conditions. These soils would be most similar in mineralogy and strength to the ACT aggregates prepared for this study, although they are natural soils. However, many other particle mineralogies have been the subject of particle breakage research (Hardin, 1985). As noted by Altuhafi & Coop (2011), the tensile resistance of individual grains (i.e. related to the mineralogy of the grain) play a critical role in the extent of particle breakage, but a

given soil mineralogy can result on different levels of particle breakage for a given stress path if the particle size distribution is considerably different. Altuhafi & Coop (2011) showed an uncemented carbonate sand with uniform graded grain size distributions exhibited more particle breakage than well-graded grain size distributions. This was also shown previously by Lee & Farhoomand (1967). Altuhafi & Coop (2001) also showed in this study that higher initial void ratios of a given particle size distribution exhibited more particle breakage than lower initial void ratio samples.

As a general rule, angular soil particles will be more susceptible to particle breakage than rounded particles (Lee & Farhoomand, 1967). It has also been found that, all other factors being equal, larger soil particles are more susceptible to particle breakage than smaller particles (Lee & Farhoomand, 1967). As explained by Lobo-Guerrero & Vellejo (2005), the effect of increased particle size on increased particle breakage is due to random flaws in the size of the particle; as the particle size increases, the probability of that the number of flaws in the particle also increases.

It is logical that stress application to a soil will have an influence on particle breakage. This includes the stress level, stress path, and time effects (Coop 1990; Lade *et al*.1996; Yamamuro & Lade, 1993). Other factors that play a role in the particle breakage would include moisture conditions (Ovalle *et al*. 2015).

Various methods to assess the extent of particle breakage during stress application have been developed over the years. Marsal (1967); Lee & Farhoomand (1967); Hardin (1985) are researchers who have developed methods of evaluating particle breakage using “before and after” comparisons of grain size distributions. As particle breakage

occurs in a loading condition, the particle size will ultimately become finer as large particles reduce in size due to the breakage. Although there are many techniques for assessing particle breakage using grain size distribution techniques, the method proposed by Hardin (1985) is one that appears frequently in the literature, mainly due to its simplicity. It is also a useful technique to adopt because it allows comparison to other studies. Hardin (1985) assumed that the breakage of particles terminated when the gradation curve of soil reached a stable condition. The final condition was achieved when all particles were smaller than 0.074 mm (sieve No. 200). The relative breakage (B_r) of soil is calculated from the following equation:

$$B_r = \frac{B_t}{B_p} \qquad (5)$$

Figure 12 shown the definition of relative breakage (B_r). The total breakage, B_t, is area between the initial and final grain size distribution curves and breakage potential, B_p, is area between the original grain size distribution curve and vertical line at 0.074mm sieve size.

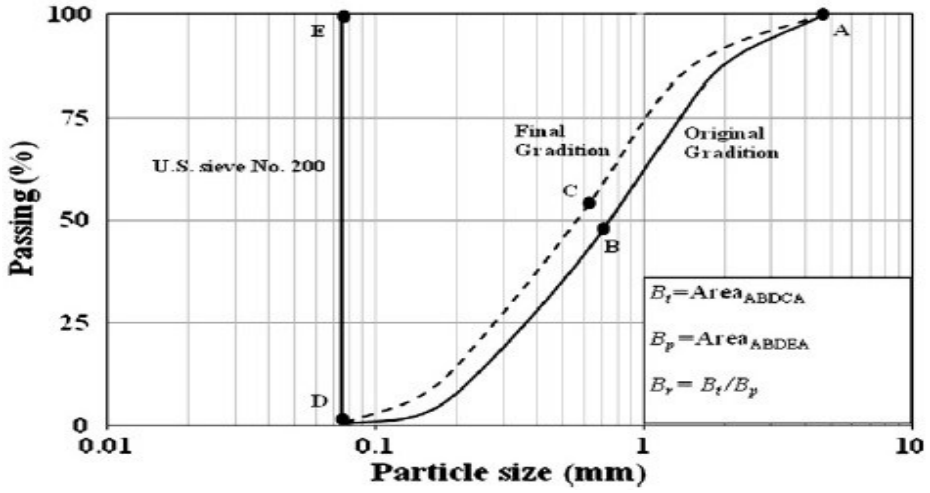

Figure 12. Definition of B_r based on the Hardin method (Shahnazari & Rezvani, 2013)

As noted by Luzzani & Coop (2002), one disadvantage of the Hardin method is that it ignores particle breakage of particle sizes less than the 0.074mm. This would be particularly important when assessing particle breakage in finer grained materials.

Although methods such as Hardin's for examining particle breakage are useful for comparison purposes, they do not provide a framework for implementing into geotechnical analyses. Various researchers have used critical state soil mechanics principles to examine particle breakage. Coop (1990) presented the results of triaxial tests on uncemented carbonate sand and showed how a unique normal compression line existed for the sand being tested (i.e. independent of triaxial test; drained vs undrained; independent of initial void ratio) and the how the degree of volume change (i.e. particle breakage) depended on the direction of the stress path. Coop (1990) showed in this work that yielding of the sand is gradual upon initial compression but after unloading and subsequent reloading, the onset of yielding is sudden at the preconsolidation pressure. Luzzani & Coop (2002) also showed when analyzing ring shear tests on the same uncemented carbonate sand run to large volumetric strains, particle breakage was still occurring (i.e. not at its critical state). The volumetric compression of the sample was shown to be directly related to particle breakage.

This approach to particle breakage as advocated by Coop (1990) and his research team is particularly useful for implementing into constitutive models for soil-structure interaction analyses. Other assessments of particle breakage for modelling applications have been developed using work methods (Miura & O'Hara, 1979; Konrad & Salami, 2017), fractal methods (Einav, 2007) and, more recently, Discrete Element Modelling (DEM) (de Bono & McDowell, 2014).

After this extensive literature review, it was concluded that:

1) Significant literature exists on particle breakage, for a variety of soil types. Although there is literature that exists on particle breakage of calcareous sands, few, if any studies, have examined particle breakage of manufactured ACT aggregates (specifically CKD derived aggregates).

2) It has been shown in the literature that grain size distribution and particle size are important factors in the extent of particle breakage observed from aggregates.

3) There are several techniques to assess the extent of particle breakage but the Hardin (1985) approach is most commonly used for comparison purposes. The Hardin approach also allows comparison to many other soil materials in the literature.

In this chapter, the susceptibility of a CKD derived ACT aggregate to undergo particle breakage is examined for various mechanical and environmental loadings. The purpose of the work is to provide a relative comparison of particle breakage for the ACT aggregate described in Chapter 3 subjected to a series of triaxial tests (drained isotropic compression, drained isotropic compression followed by drained axial shear) as well as freeze thaw tests. The influence of aggregate size/gradation on the particle breakage is also assessed using the Hardin method. Results are compared to various other particles in the literature.

4.2 Materials

The testing performed in this chapter used the same cement kiln dust material discussed in Chapter 3. In summary, the material was obtained from a Lafarge cement plant in

Brookfield (Nova Scotia, Canada) in August 2014. The CKD consists of calcium, iron, silica, aluminum, magnesium and potassium oxides, with 42% CaO content being the key component of the accelerated carbonation technology for producing the aggregate.

The pelleting process described in Chapter 3 was modifying slightly in an attempt to produce a stronger aggregate. Pelleting of ACT aggregates consisted of premixing 400g (dry mass) of CKD with 130g water using a laboratory paddle mixer. During this phase of the mixing process, CKD with water mixed for 45~60 seconds at 50 rpm speed mixing and then 30~60 seconds at 120 rpm speed mixing. Subsequently, an additional 60g of CKD was added during 120 rpm speed mixing and then 40g CKD was added to mixer (depend upon the aggregate surface water condition); then mixed for 30 seconds at 50 rpm to produce more rounded aggregates. The mix was then placed in a rotating drum with CO_2 saturation for 15 minutes at 50 rpm to make the aggregate. The ACT aggregates in this study were air-cured at 20 ± 2°C and ~25% relative humidity conditions in a lab for at least 28 days prior to being subjected to any testing. As noted in Chapter 3, this air curing is representative of the likely field curing conditions that would occur.

In this chapter, three different particle size distributions were assessed. The full particle size distribution referred to as “entire sample” produced from the ACT process was used initially for testing. A typical grain size distribution is shown in Figure 13. Additional aggregate was prepared using the same techniques for the entire sample but the aggregate was for the segregated into two distinct size fractions (5mm-2.5mm and 2.5mm to 1.25mm) after curing. This was accomplished by passing the material through the 5 mm sieve followed by the 2.5 mm sieve followed by the 1.25 mm sieve. Material

retained on the 5 mm sieve and passing the 1.25 mm sieve was discarded. Material retained on the 2.5 mm sieve is referred to as the "5mm-2.5mm" sample and the material retained on the 1.25 mm sieve is referred to as the "2.5mm-1.25mm" sample.

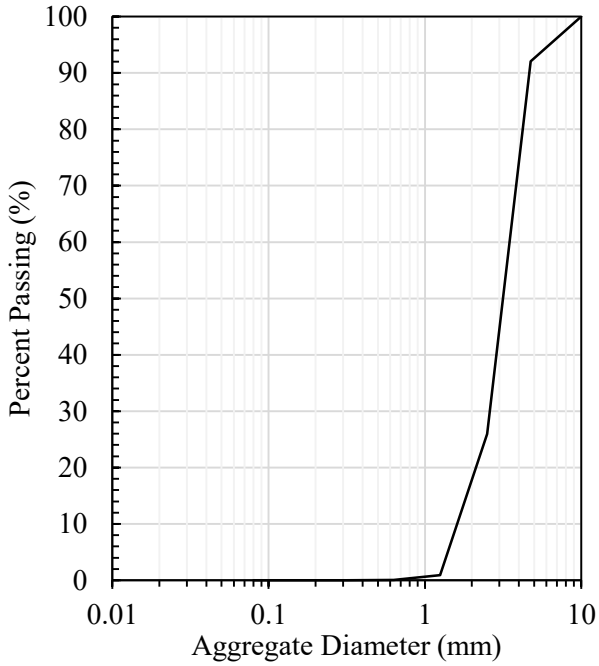

Figure 13. Typical ACT aggregate grain size distribution (entire sample)

4.3 Test Procedures

4.3.1 Single Aggregate Pellet Strength

To provide an initial assessment of individual particle strength, a single pellet compressive strength test (ASTM D4179-11, 2011a), as described in Chapter 3, was used. Ten (10) samples were taken from the two ACT aggregate grain sizes prepared (i.e. 2.5mm-1.25 mm; 5mm-2.5mm) and subjected to single pellet compressive strength tests. The mean value of the strength was reported. Given that the majority of the entire sample fell within these grain sizes, other particle sizes were not tested. Particle strengths were measured at 7, 15 and 27 days of air-curing.

4.3.2 Drained Isotropic Triaxial Compression Tests

To assess the extent of particle breakage of the ACT aggregate during drained isotropic triaxial compression, the three grain sizes of the ACT aggregate were subjected to isotropic compression tests similar to that described in Chapter 3. For the entire sample, compared a two subsamples were taken of the prepared aggregate; one was submitted to a grain size analysis and the second used in the triaxial compression tests. In summary, the given aggregate size was compacted in a split mould (70mm diameter x 150mm high) and subjected to saturation under 35 Kpa (5 psi) effective confining pressure in a triaxial cell. The sample was then subjected to consolidation under the desired effective confining pressure (600, 800, 1000, 1200 or 1400 kPa) to produce the isotropic compression conditions desired. The 1400 kPa represent the limit of the cell pressure available. The test progressed until the specimen reached equilibrium in a drained state at the desired effective consolidation stress. After this was achieved the grain size curve of the sample was determined in order to assess the extent of particle breakage that occurred. For the 5mm-2.5mm size and 2.5mm-1.25mm size tests, the grain size distributions only after the tests were performed. The grain size distributions of both samples were plotted and compared visually and the Hardin parameter calculated from the grain size curves.

4.3.3 Drained Isotropic Compression, Drained Axial Shear Triaxial Tests

To assess the extent of particle breakage of the ACT aggregate under shearing conditions, the three grain sizes of the ACT aggregate were subjected to drained isotropic compression followed by drained axial shear. Samples were prepared similar

to that described in the previous chapter. In summary, the given aggregate size was compacted in a split mould and subjected to saturation under an effective confining pressure of 35 kPa (5psi). The sample was then subjected to consolidation under the desired effective confining pressure (600, 800, 1000, 1200 or 1400 kPa) and subsequently sheared drained under an axial displacement rate of 1.5 mm/min. Axial loading was terminated at 15% axial strain to provide a common strain level to compare breakage to for each test. Volume changes were not recorded during testing. The loading frame and triaxial test cell is shown in Figure 14. Similar to the triaxial compression tests described in the previous section, grain size distributions were compared before and after testing and Hardin parameter calculated.

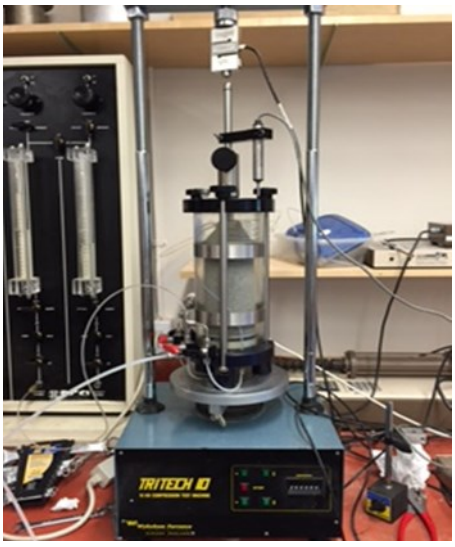

Figure 14. Triaxial test apparatus

4.3.4 Freeze/Thaw Durability Testing

Freeze/thaw durability testing, similar to that described in Chapter 3 was performed on the three ACT aggregate sizes. To summarize, after the aggregate sample was soaked

in water for 4h, they were surface dried for approximately 15min. The test aggregate samples were then subjected to 10 or 20 freeze–thaw cycles that included freezing to −17·5 ± 2·5°C for 24 h and then thawing in a water bath at room temperature (~20 ± 2°C) for 4 h. Freeze-thaw cycle tests were performed in duplicated in Dalhousie University soil lab (BSI BS EN 13055-4, 2016). At the end of the freeze–thaw cycles, the samples were subjected to grain size analysis to compare particle size distributions before and after the freeze–thaw cycling. For comparison to triaxial compression and/or shear testing. Hardin breakage parameters were calculated at the end of each test.

4.4 Test Results

4.4.1 Single Aggregate Pellet Strength

As shown in Table 12 and Figure 15, particle strengths for the two sizes increased as the curing time increased. The 5mm-2.5mm aggregate achieved strengths of 1.8 MPa, 2.6 MPa, and 2.9 MPa after 7, 15, and 27 days of curing respectively. The 2.5mm-1.25mm aggregate achieved strengths of 2.0 MPa, 2.8MPa and 3.0 MPa after 7, 15, and 27 days of curing respectively. For these simple particle strength tests, there appears to be little, if any, difference in particle strength between the two particle sizes tested.

Table 12. Average single pellet strengths of different aggregate sizes (n=10)

ACT aggregate size	Curing Time (days)	Average strength (MPa)
5-2.5mm	7	1.8
	15	2.6
	27	2.8
2.5-1.25mm	7	2.0
	15	2.8
	27	3.0

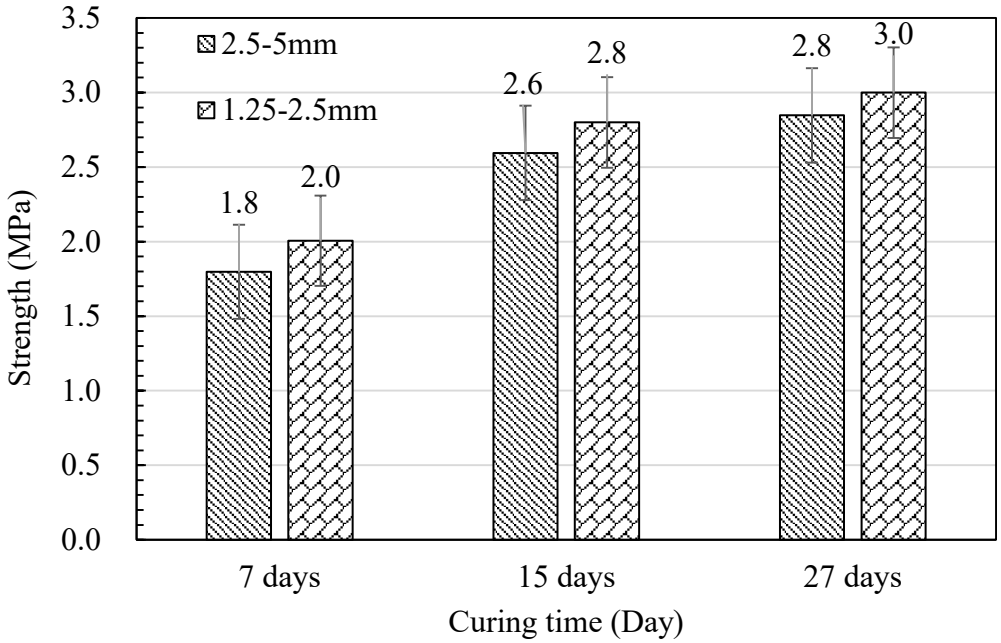

Figure 15. Single pellet strength at different curing times

4.4.2 Drained Isotropic Triaxial Compression Testing

Entire Sample Particle Size

Figure 16 shows the particle size distributions for the entire sample size of ACT aggregate before and after the drained isotropic triaxial compression testing for the five effective confining stresses employed (600, 800, 1000, 1200, 1400, and 1600 kPa). As seen from the Figure 16, the grain size distributions of the sample visually changed little during these tests. At the higher confining pressures (1200 kPa and 1400 kPa), the grain size did change slightly as is evident by the increase in the finer fraction of the soil. The resulting Hardin relative breakage (B_r) for the entire sample size of ACT aggregate are shown in Table 13. Similar to the visual observations noted above, Br increased as the confining pressure increased; the greatest increase occurring from 1000 to 1200 kPa.

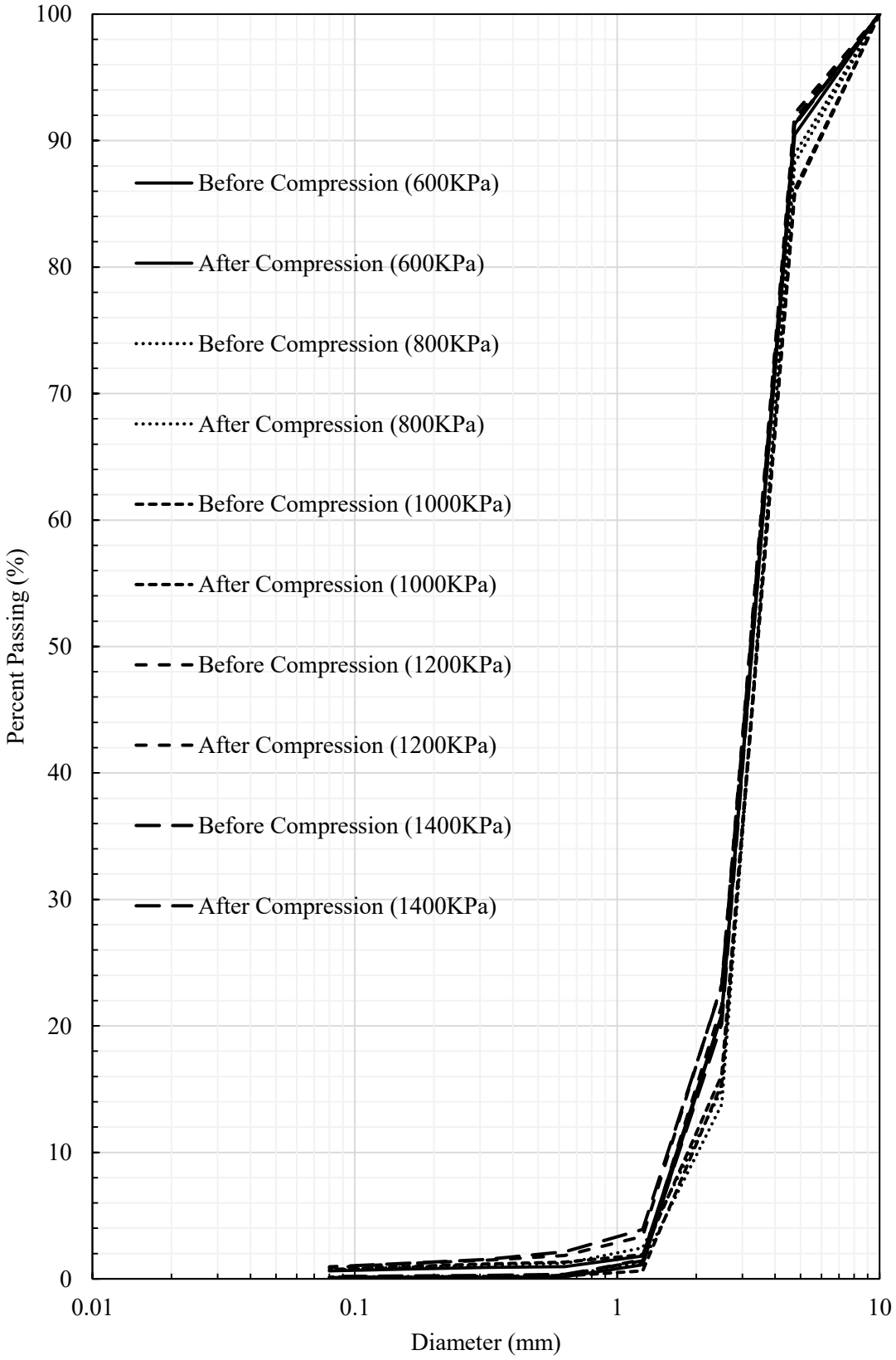

Figure 16. Before and after particle size distributions for the entire ACT aggregate sample (triaxial compression).

Table 13. Comparison of the relative breakage (B_r) obtained at different confining pressures in triaxial compression tests from the three different particle sizes

Sample	Effective Confining Pressure (kPa)	Hardin Relative Breakage $B_r = B_t/B_p$
Entire sample	600	0.0067
	800	0.0069
	1000	0.0076
	1200	0.0133
	1400	0.0160
5mm-2.5mm	600	0.0088
	800	0.0093
	1000	0.0122
	1200	0.0158
	1400	0.0198
2.5mm-1.25mm	600	0.0042
	800	0.0056
	1000	0.0063
	1200	0.0079
	1400	0.0100

5mm-2.5mm Particle Size

Figure 17 shows the particle size distributions for the ACT aggregate before and after the drained isotropic triaxial compression testing for the 5mm-2.5mm aggregate for the five effective confining stresses employed (600, 800, 1000, 1200, and 1400 kPa). The initial particle size distribution is one straight line as only are particle size in present in this sample. As seen from the Figure 17, the grain size distributions of the sample visually changed more than that for the entire sample during these tests. It visually appears when examining these grain size plots that there is a more pronounced effect on particle crushing compared to that of the entire grain size distribution and that as the confining pressure increased, the breakage appeared to also increase (i.e. appearance of finer grain fraction). The resulting relative breakage for this size as shown in Table 13 confirm this observation. It is also noted that the

breakage parameters found for this aggregate size were higher than that of the entire sample. This is consistent with Francesca & Giulia (2013). Altuhafi & Coop (2011) also showed how larger particle size and grain size uniformity can result in increases in particle breakage.

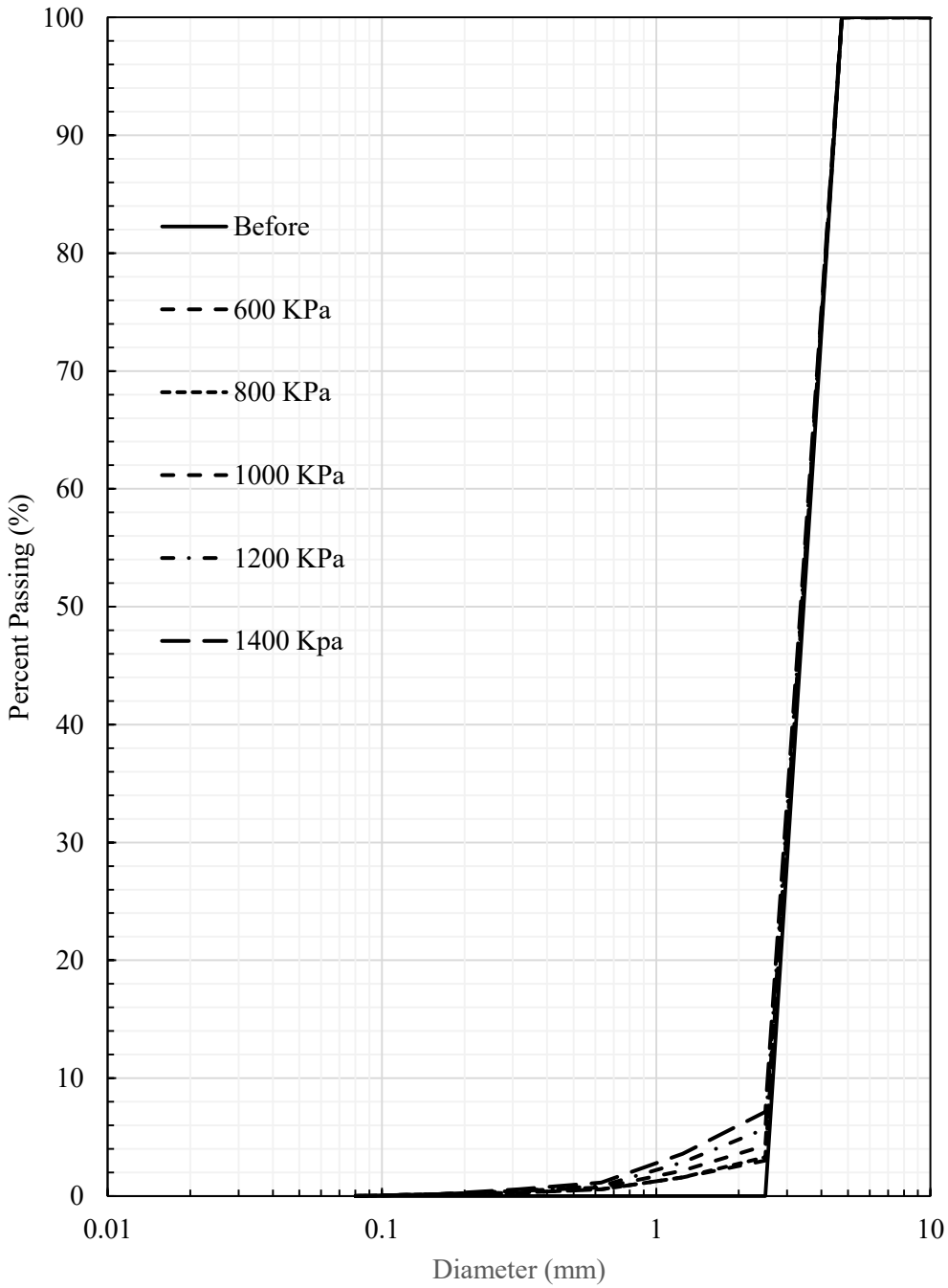

Figure 17. Before and after particle size distributions for the 5mm-2.5mm ACT aggregate sample (triaxial compression).

2.5mm-1.25 mm Particle Size

Figure 18 shows the particle size distributions for the ACT aggregate before and after the drained isotropic triaxial compression testing for the 2.5mm-1.25mm aggregate for the five effective confining stresses employed (600, 800, 1000, 1200, and 1400 kPa). As with the 5mm-2.5mm material, the initial particle size distribution is one straight line as only one particle size in present in this sample. As seen from the Figure 18, the grain size distributions of the sample visually changed less than the 5mm-2.5mm sample and that of the entire sample during these tests. It does visually appear that there is some minor particle breakage as the confining pressure increased. The resulting particle breakage for this size as shown in Table 13 confirm this observation. It is also noted that the breakage parameters found for this size aggregate were lower than that of the entire sample and the 5mm-2.5 mm sample. This is perhaps not surprising when comparing to the entire sample as it is likely the large particle breakage occurred in the 5mm-2.5 mm fraction of the sample.

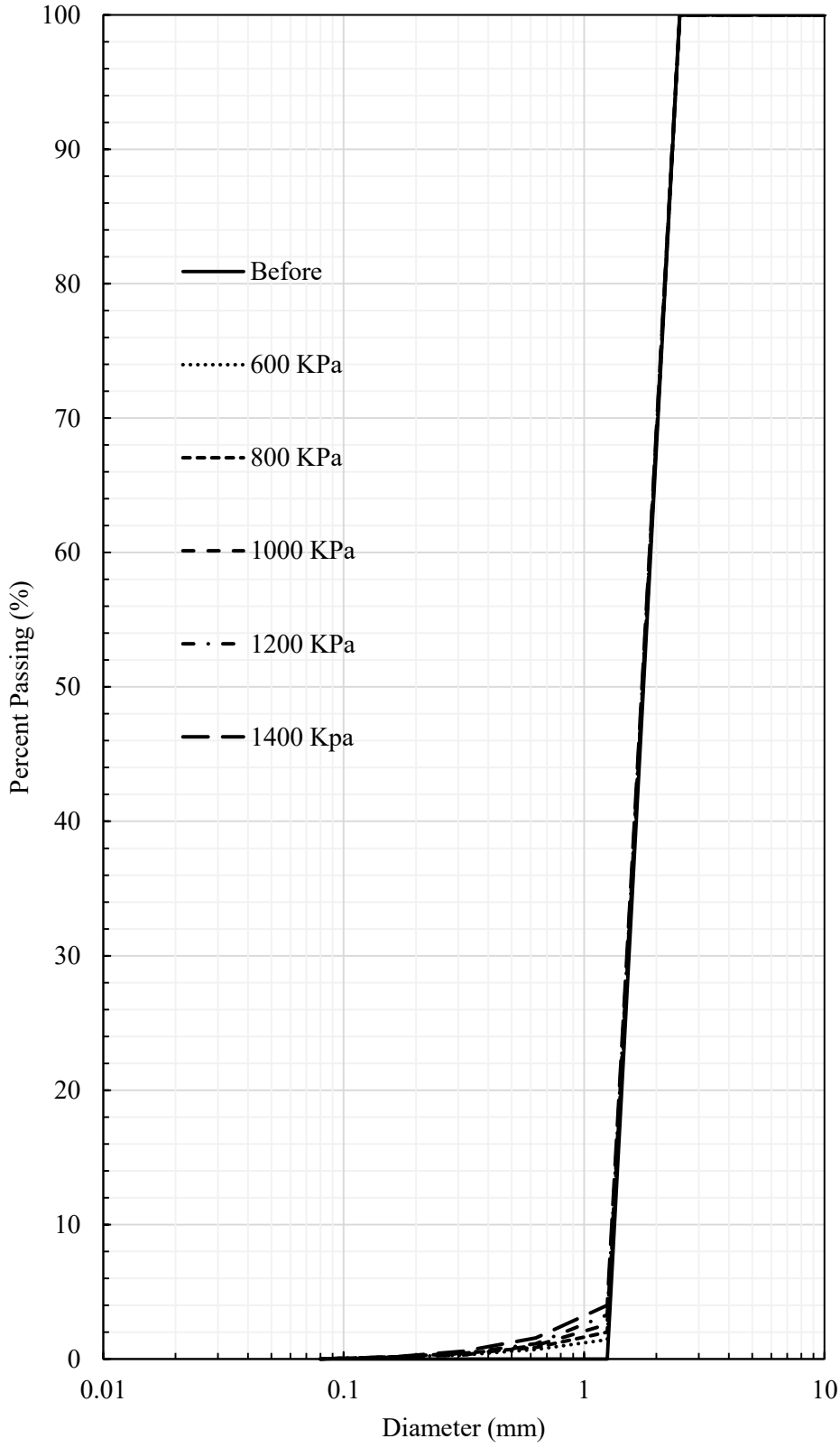

Figure 18. Before and after particle size distributions for the 1.25-2.5mm ACT aggregate sample (triaxial compression).

The results of Table 13 are summarized in graphical form below in Figure 19. As previously discussed, the particle breakage (appears to be greatest for the 5mm-2.5 mm sample due to the uniform grain size distribution (relative to the entire sample). Also noticeable from Figure 19 is the distinct "kink" in the curve at the 800-1000 kPa range of confining pressure. This is likely the onset of yield of the particles at this confining pressure. Luzzani & Coop (2002) showed a similar behavior, albeit with samples loaded to critical state conditions. Luzzani & Coop (2002) looked at a variety of stress paths and used the mean effective stress to show this relationship. The discussion section will further discuss a unique relationship between mean effective stress and the onset of significant breakage in the particles.

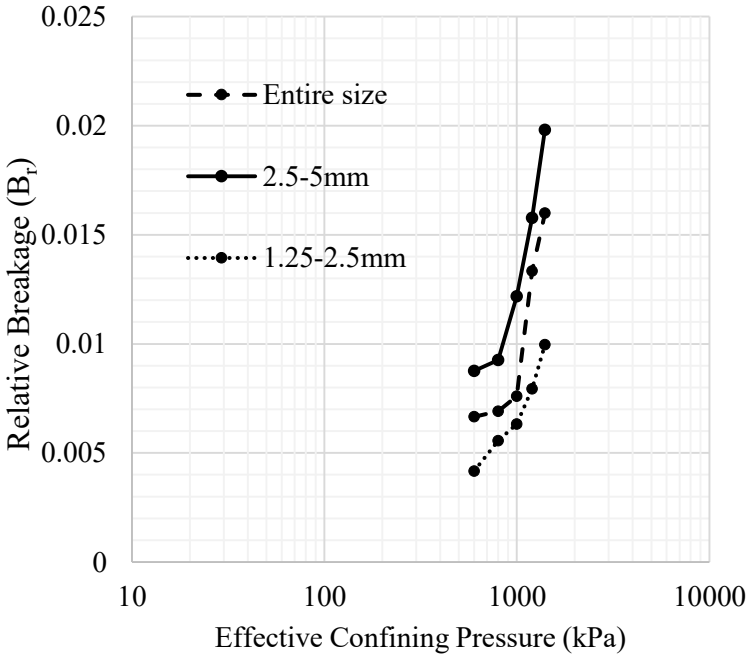

Figure 19. Summary of the variation of B_r versus effective confining pressure for triaxial compression tests.

4.4.3 Drained Isotropic Compression, Drained Axial Shear Triaxial Test

The result of the drained axial shear triaxial tests are provided in appendix B, C and D for reference. The results in this section focus mainly on the particle breakage during shear.

Entire Sample Particle Size

Figure 20 shows the particle size distributions for the ACT aggregate before and after the drained triaxial shear testing for the entire sample particle size distribution of the ACT aggregate for the five effective confining stresses employed (600, 800, 1000, 1200, 1400, and 1600 kPa). As seen from the Figure 20, compared to the isotropic triaxial compression tests for the entire sample, there was noticeably more particle breakage from the shear testing. There also appears to be more particle breakage increases as the confining pressure was increased. The resulting relative breakage for the ACT aggregate are shown in Table 14. Similar to the visual observations noted above, the Hardin parameter increased as the confining pressure increased. Also to note from examining this table is the higher values of Br relative to the isotropic triaxial compression tests reported in Table 13. As will be discussed later, this is due to the higher mean stress in the samples relative to isotropic triaxial compression tests and the shear being generated in the samples.

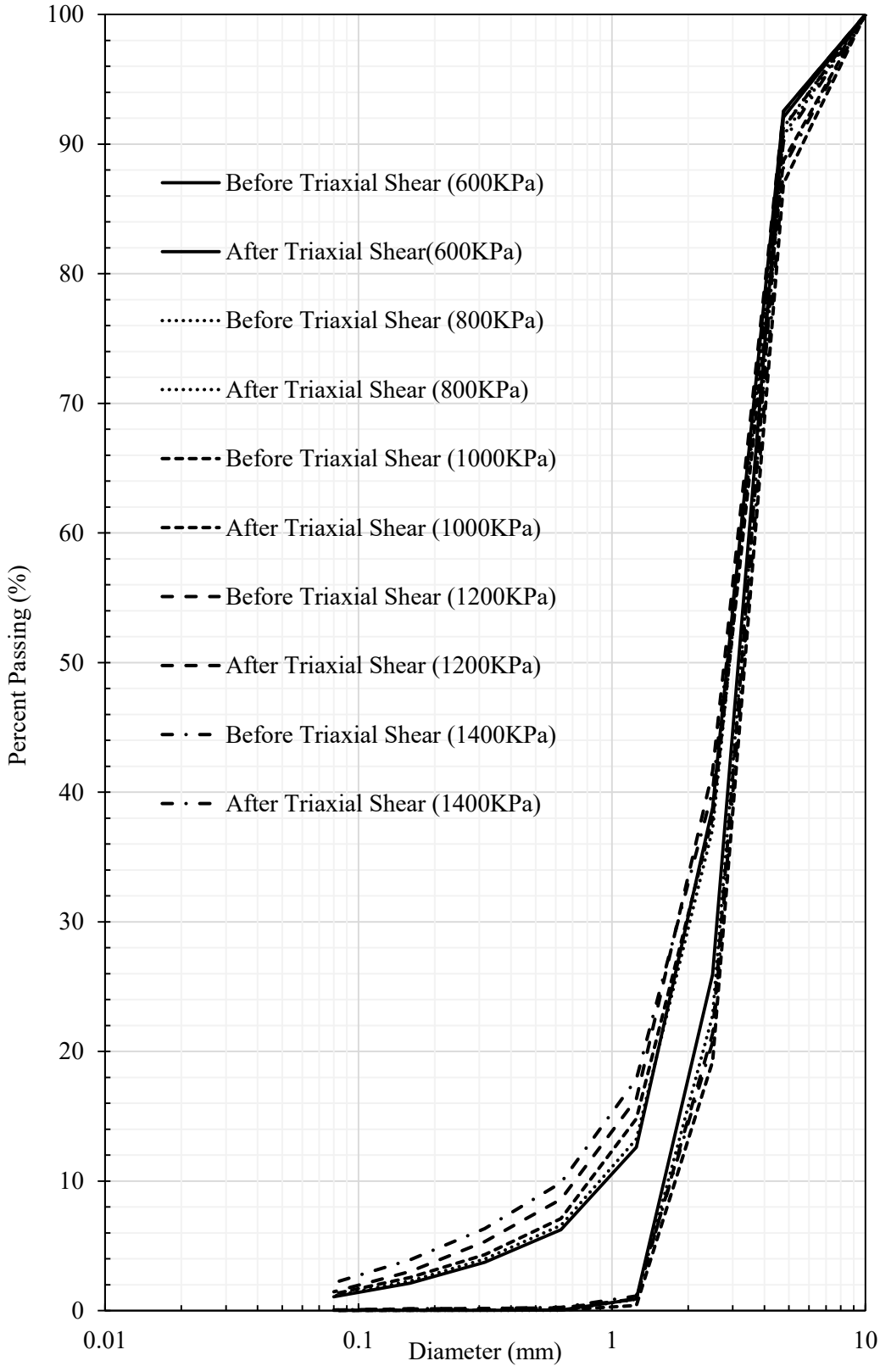

Figure 20. Before and after particle size distributions for the entire size ACT aggregate sample (triaxial shear test).

Table 14. Relative breakage (B_r) for the three different particle sizes examined.

Sample	Effective Confining Pressure (kpa)	Relative Breakage (B_r)
Entire size	600	0.0593
	800	0.0639
	1000	0.0775
	1200	0.0858
	1400	0.0924
2.5-5mm	600	0.0669
	800	0.0783
	1000	0.0962
	1200	0.1010
	1400	0.1194
1.25-2.5mm	600	0.0382
	800	0.0409
	1000	0.0489
	1200	0.0576
	1400	0.0726

5mm-2.5mm Particle Size

Figure 21 shows the particle size distributions for the ACT aggregate before and after the drained triaxial shear testing for the 5mm-2.5mm aggregate for the five effective confining stresses employed (600, 800, 1000, 1200, and 1400 kPa). The initial particle size distribution is one straight line as only particle size in present in this sample. As seen from the Figure 21, the grain size distributions of the sample visually changed more than that for the entire sample during these tests, similar to that observed for the isotropic triaxial compression tests. It visually appears when examining these grain size plots that there is a more pronounced effect on particle crushing compared to that of the entire sample and that as the confining pressure increased, there was the appearance of a finer grain fraction. The resulting relative breakage for the ACT aggregate as shown

in Table 14 confirm this observation. It is also noted that the Br values found for this size aggregate were higher than that of the entire sample and that the values of Br are higher than that for the isotropic triaxial compression tests.

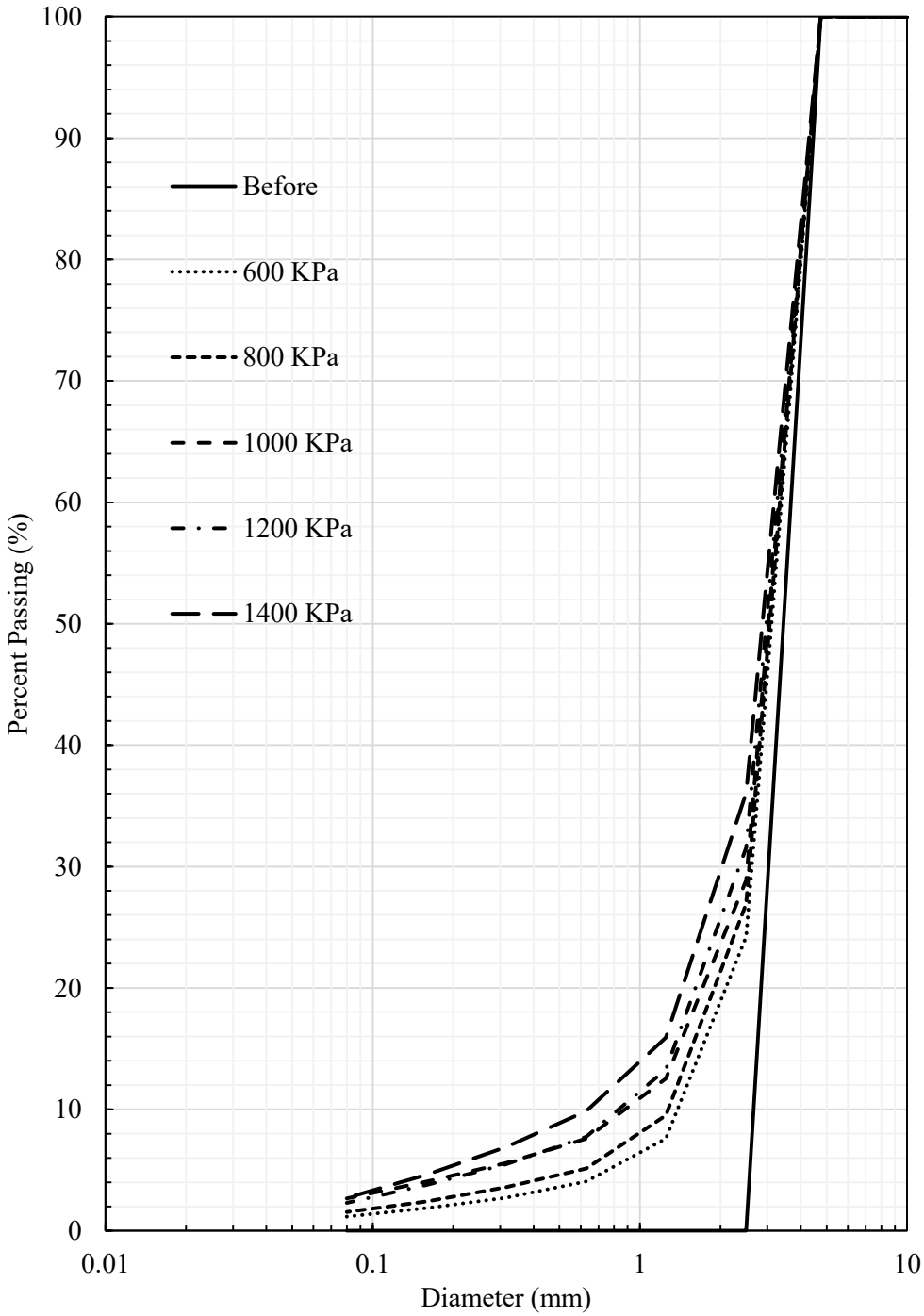

Figure 21. Before and after particle size distributions for the 5mm - 2.5mm size ACT aggregate sample (triaxial shear test).

2.5mm-1.25 mm Particle Size

Figure 22 shows the particle size distributions for the 2.5mm-1.25mm ACT aggregate before and after the drained triaxial shear testing, for the five effective confining stresses employed (600, 800, 1000, 1200, and 1400 kPa). As with the 5mm-2.5mm material, the initial particle size distribution is one straight line as only particle size in present in this sample. As seen from the Figure 22, the grain size distributions of the sample visually triaxial shear changed less than both the 5mm-2.5mm sample and that of the entire sample during these tests. It does visually appear that there is some minor particle breakage as the confining pressure increased, albeit less than the other two sizes. The resulting relative breakage (B_r) for the 2.5mm-1.25mm ACT aggregate, as shown in Table 14, confirm this observation. It is also noted that the particle breakage found for this size aggregate were lower than that of the entire sample and the 5mm-2.5 mm sample. This is perhaps not surprising as it is likely the large particle breakage occurred in the 5mm-2.5 mm fraction of the sample. Also noted is the relative increase in Br compared to triaxial compression testing. Again, not surprising given the increase in mean stress.

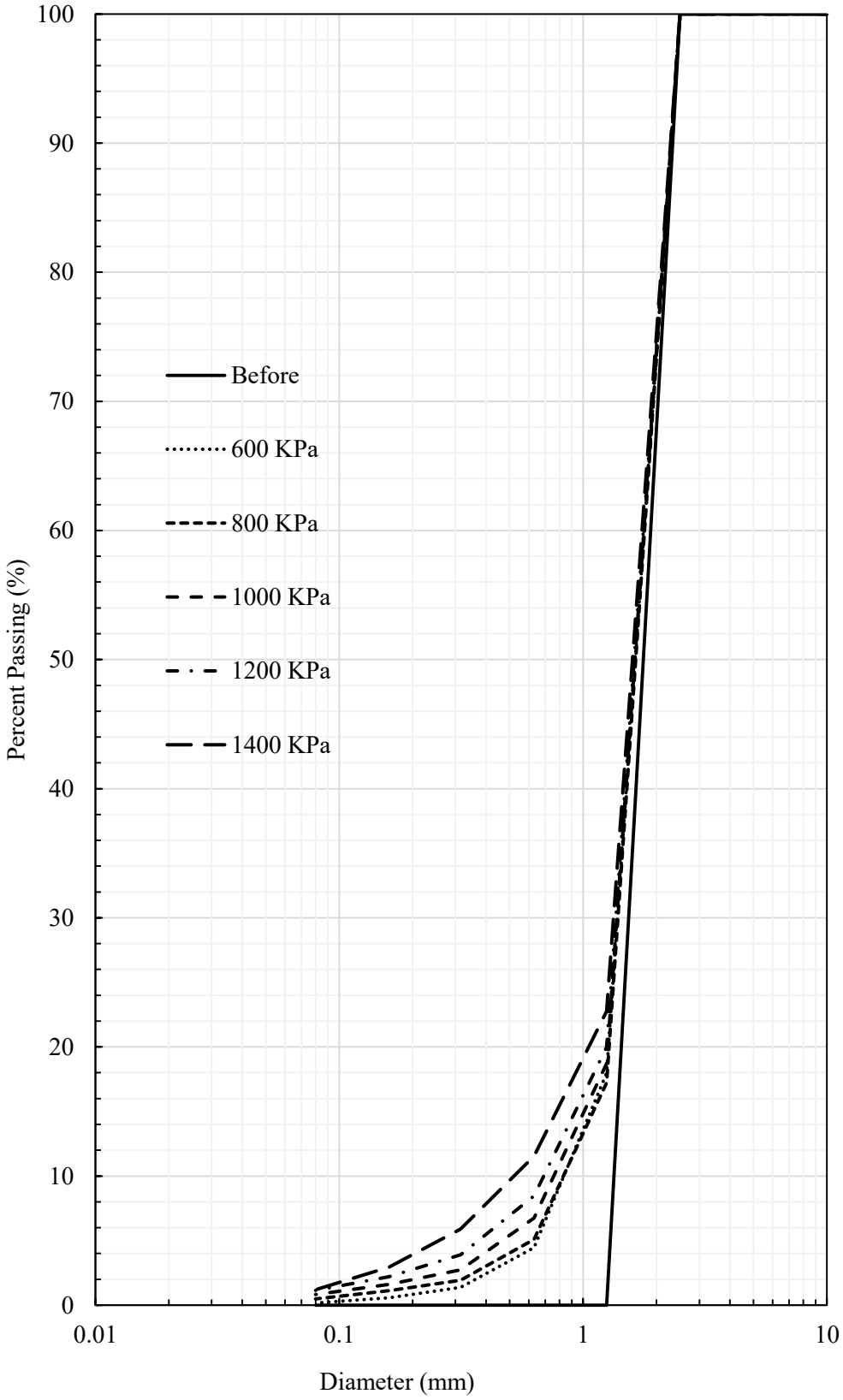

Figure 22. Before and after particle size distributions for the 1.25-2.5mm size ACT aggregate sample (triaxial shear test).

All results from Table 14 are summarized below in Figure 23. As previously discussed, the B_r appears to be greatest for the 5mm-2.5 mm sample due to the uniform grain size distribution (relative to the entire sample) and the increase as the particle size of the sample (relative to the 2.5 mm-1.25 mm sample). Unlike the triaxial compression tests, there was no noticeable distinct "kink" in the curve at a given confining pressure. One noticeable difference between the shear tests and compression tests would be the much higher values of B_r for the shear tests. This was also observed by Lee & Farhoomand (1967). The discussion portion of this chapter will discuss further the relationship between mean effective stress and the onset of significant breakage in the particles.

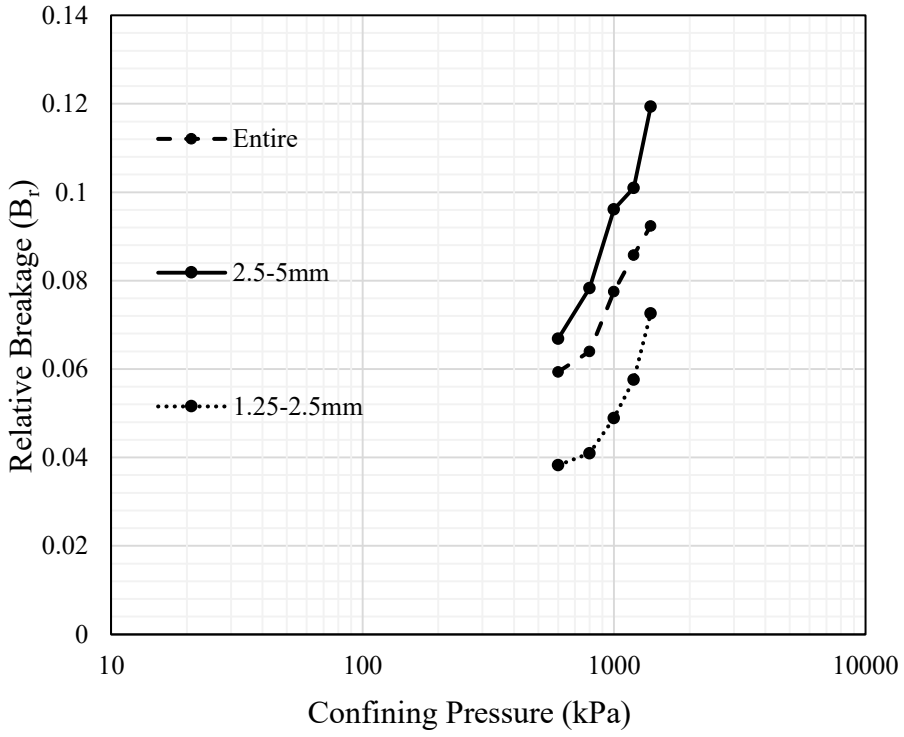

Figure 23. Summary of the variation of B_r versus effective confining pressure for triaxial shear tests.

4.4.4 Freeze/Thaw Cycle Effect on Particle Breakage

Freeze-thaw cycle tests were performed in duplicate and Hardin breakage parameters were calculated the average data of before and after freeze-thaw cycle sieve analysis. Figure 24 shows the grain size distribution of the entire sample before and after freeze/ thaw cycling testing. After 10 cycles of f/t it is apparent that the grain size distribution of the entire sample has a finer grain size distribution and after 20 cycles of F/T, this particle size became even finer. The percent passing the 2.5 mm sieve has increased the most in both instances, indicating the larger portion of the sample may be exhibiting more breakage. This phenomena of particle breakage of the larger size aggregate can be examined further when examining Figures 25 and 26. It can be seen that when the 2.5mm-5mm and 1.25mm-2.5mm size particles were isolated, the 2.5mm-5mm size fraction exhibited significantly more breakage than that of the 1.25mm-2.5mm size. The 1.25mm-2.5mm grain size curve visually changed little.

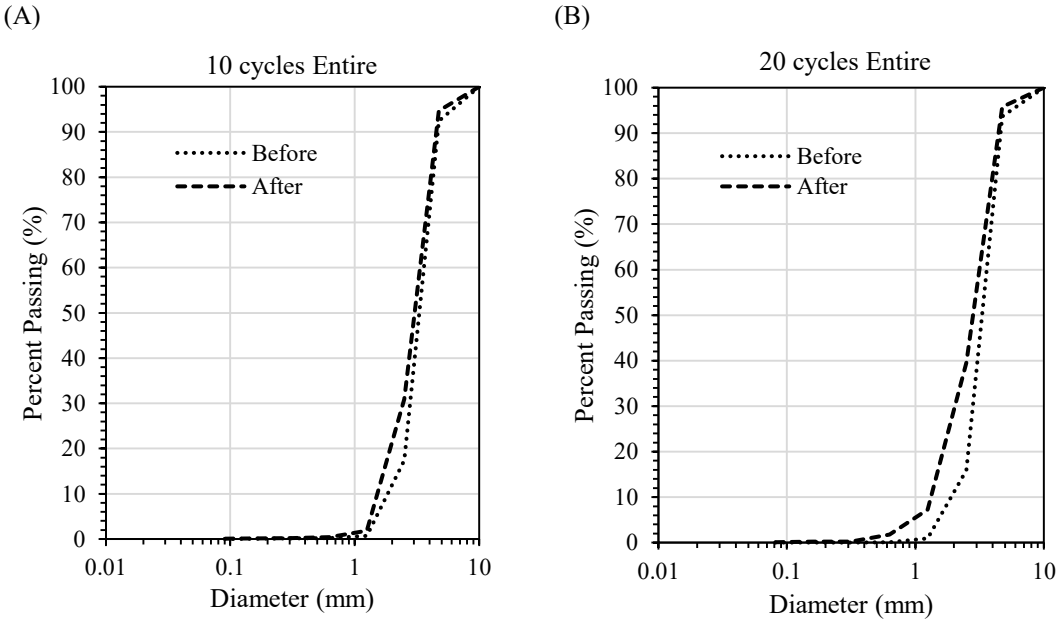

Figure 24. Entire cycles ACT aggregate sample sieve analysis result, before and after 10-20 freeze/thaw

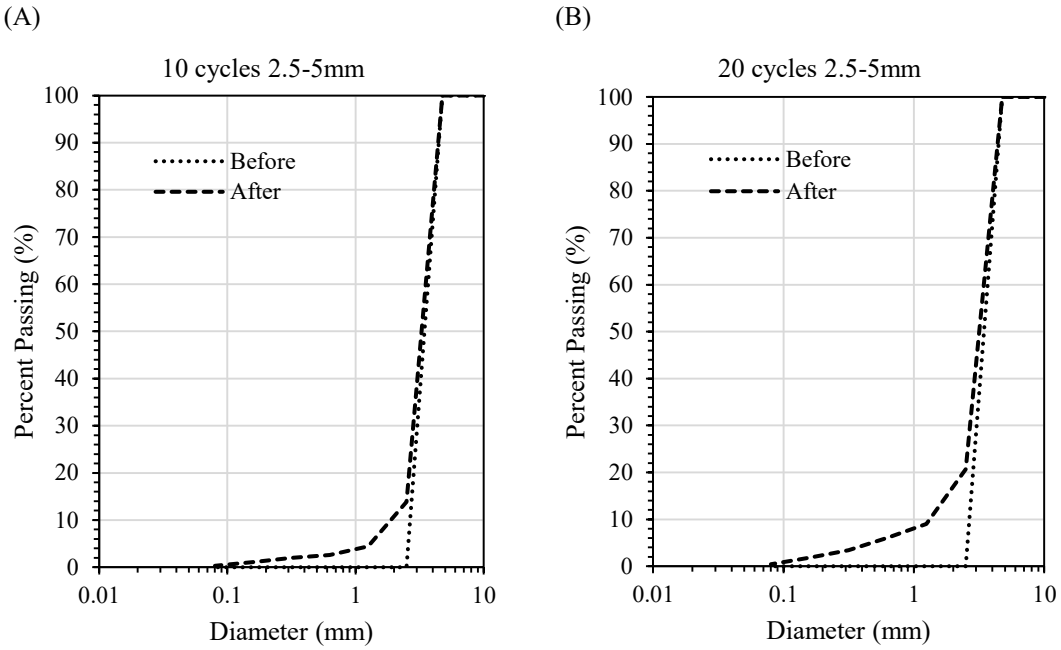

Figure 25. 2.5-5mm cycles size ACT aggregate sample sieve analysis result, before and after 10-20 freeze/thaw

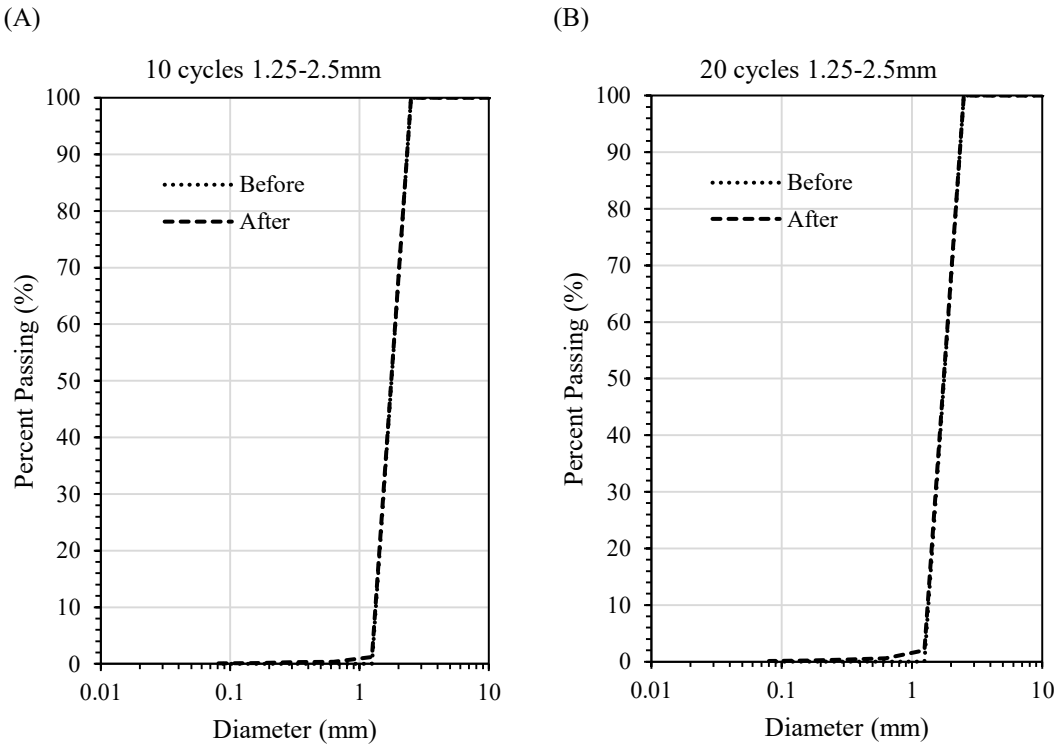

Figure 26. 1.25-2.5mm cycles size ACT aggregate sample sieve analysis result, before and after 10-20 freeze/thaw

Although particle breakage are usually used for mechanical loading applications, it is interesting to calculate B_r for the freeze/thaw cycle tests (see Table 15 and Figure 27). The values of B_r corresponded with the visual observations of the grain size curves (more breakage with f/t cycles at 20 than 10; at a given f/t/ cycle, breakage increases 5mm-2.5mm>entire sample>2.5mm-1.25mm).

Table 15 Relative breakage (B_r) as calculated from freeze-thaw cycle tests.

Sample	Freeze/thaw cycles	Relative breakage (B_r)
Entire size	10 cycle	0.032
	20 cycle	0.060
2.5-5mm	10 cycle	0.041
	20 cycle	0.067
1.25-2.5mm	10 cycle	0.003
	20 cycle	0.005

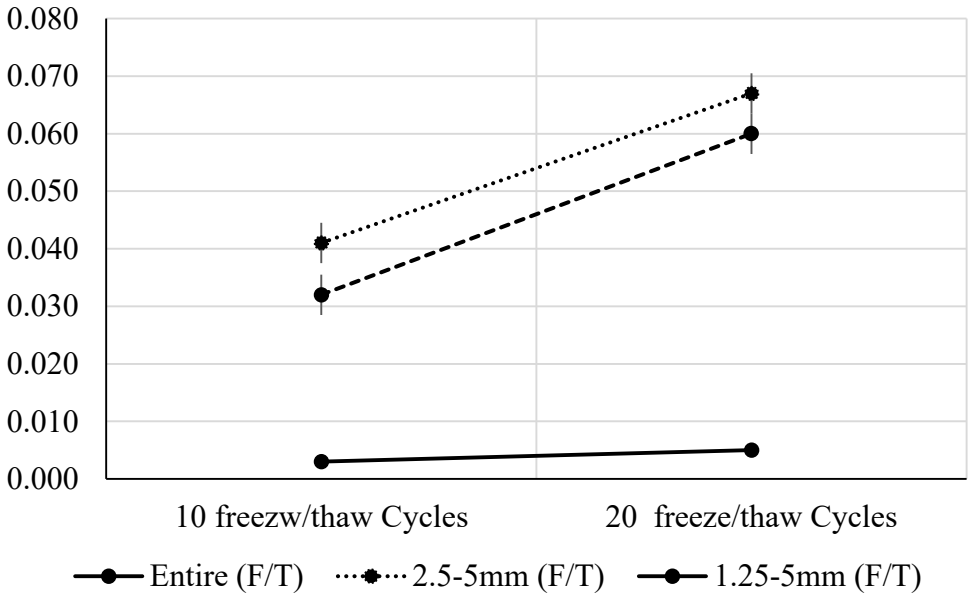

Figure 27. Relative breakage sample, Br, calculated from 10-20 cycles freeze-thaw for the three aggregate particle sizes.

4.5 Discussion

Particle Breakage Comparison between Triaxial Compression, Triaxial Shear, and Freeze-Thaw Testing

It is useful to compare the particle breakage obtained from the triaxial compression, triaxial shear, and freeze-thaw cycles testing to ascertain the loading conditions that ACT aggregates would be susceptible to particle breakage. Figure 28 shows the values of Br obtained from these three different test methods. For ease of comparison, results are presented in terms of octahedral stress, ρ'. Since triaxial compression and triaxial shear tests were performed under the same effective confining pressures, the use of octahedral stress, ρ', allows the "additional" axial stress to be accounted for when examining stresses. For the purpose of this thesis, the octahedral stress at the end of the 15% strain level (i.e. termination of the test) was used. It should also be noted that the f/t tests were performed under "zero external octahedral stress" conditions and hence the shading observed on Figure 28 represents the range of B_r values for the 10 and 20 f/t cycles for each particle size.

As previously discussed, it is apparent that for the various triaxial tests, the influence of shear resulted in a higher the amount of particle breakage (i.e. when comparing similar octahedral stress). As discussed by Coop (1990), the true measure of particle breakage is obtained from critical state conditions (which were not reached in these tests) and hence this must be remembered when examining these test results. It is noted that for a given loading condition, the 5mm-2.5mm aggregate underwent more relative breakage (B_r) than that of the 2.5mm-1.25mm aggregate. When one examines the freeze/thaw cycle test results relative to the triaxial compression and triaxial shear

results, it is interesting to see that the particle breakage from freeze/thaw cycle testing for the entire sample and 5mm-2.5 mm size corresponds to much higher particle breakage than triaxial compression testing but similar to slightly lower particle breakage as that under triaxial shear. This suggests that environmental factors such as f/t cycle may be as important a consideration in application as that compared to loading conditions. In contrast, the particle breakage of the 2.5mm-1.25mm aggregate after 20 cycles of freeze/thaw is relatively small and similar in magnitude to the same size aggregate under triaxial compression test conditions.

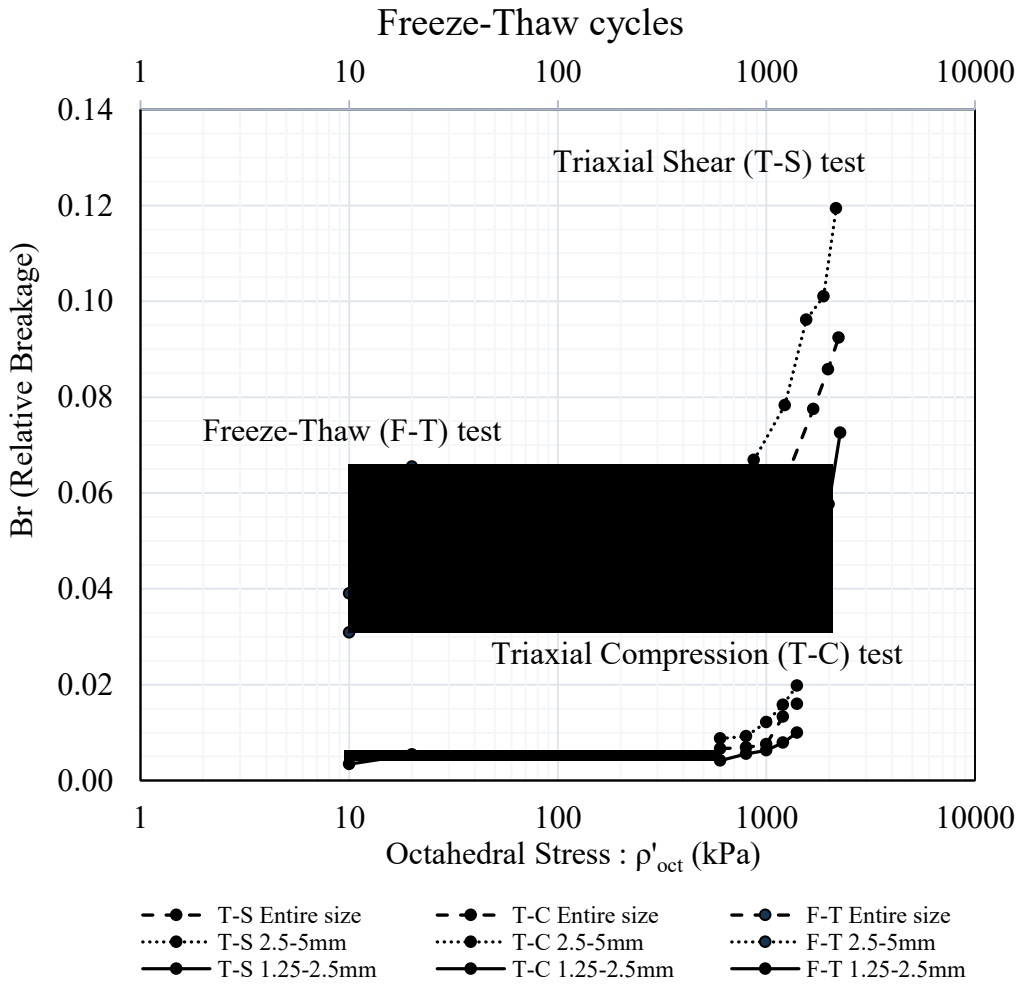

Figure 28. Relative breakage (B_r) vs octahedral stress (ρ') or number of freeze-thaw cycles.

Comparison of ACT Aggregate Particle Breakage to Other Studies

Many previous particle breakage studies exist in the literature breakage examining the influence of loading, mineralogy, and particle characteristics. Even though there are many different approaches to assessing particle breakage, it is useful to try, at least from a qualitative standpoint, to compare particle breakage obtained from this study to that of previous studies. For the purposes of this study, calcareous sands studied by Shipton & Coop (2012) (using data from Coop, 1990) and Shahnazari & Rezvani (2013) as well as predominantly silica sands tested by Mun & McCartney (2017) are used as reference materials. The silica sand tested by Mun & McCartney (2017) is relatively durable compared to the calcareous sands tested by Coop and his coworkers.

For this thesis, some values for B_r were estimated visually from plots in the various research paper and hence this may lead to same discrepancy. However, from a qualitative perspective, approximations were deemed sufficient. Also to note is that the results of Shipton & Coop (2012) and some of Shahnazari & Rezvani (2013) were a mix of isotropic compression tests and drained triaxial shear tests. As well, the tests by Shipton & Coop (2012) were run to higher strain levels than this study (i.e. would account for more particle breakage).

Figure 29 shows Br values for the various studie. Also shown on Figure 29 are the results for the 5mm-2.5mm aggregate and the 2.5mm-1.25mm aggregate. The results of the entire sample always fell between these two samples and hence are not included on Figure 29. As shown on Figure 29, at a given B_r, it took significantly more mean stress to achieve the same particles breakage Mun & McCartney (2017) as compared to the ACT aggregate in this study. This is not surprising given the relative differences in

mineralogy and individual particle strengths of the aggregates. If we compare the ACT aggregate to the carbonate sand of results for the same Br it can be seen that similar or more mean stress is required to achieve a similar particle breakage as that in this study. This is somewhat encouraging in that calcareous sands have shown to be adequate materials for construction projects in geotechnical applications provided loading and/or strain level is limited to control particle breakage. Given that the ACT aggregate is a manufactured aggregate, further modifications to aggregate production process could possibly make it more durable and less susceptible to particle breakage. This is outside the scope of this study but does provide room for thought given the sustainable aspects associated with ACT aggregate (i.e. carbon sequestration, waste material usage and reduction of quarrying for aggregate supply).

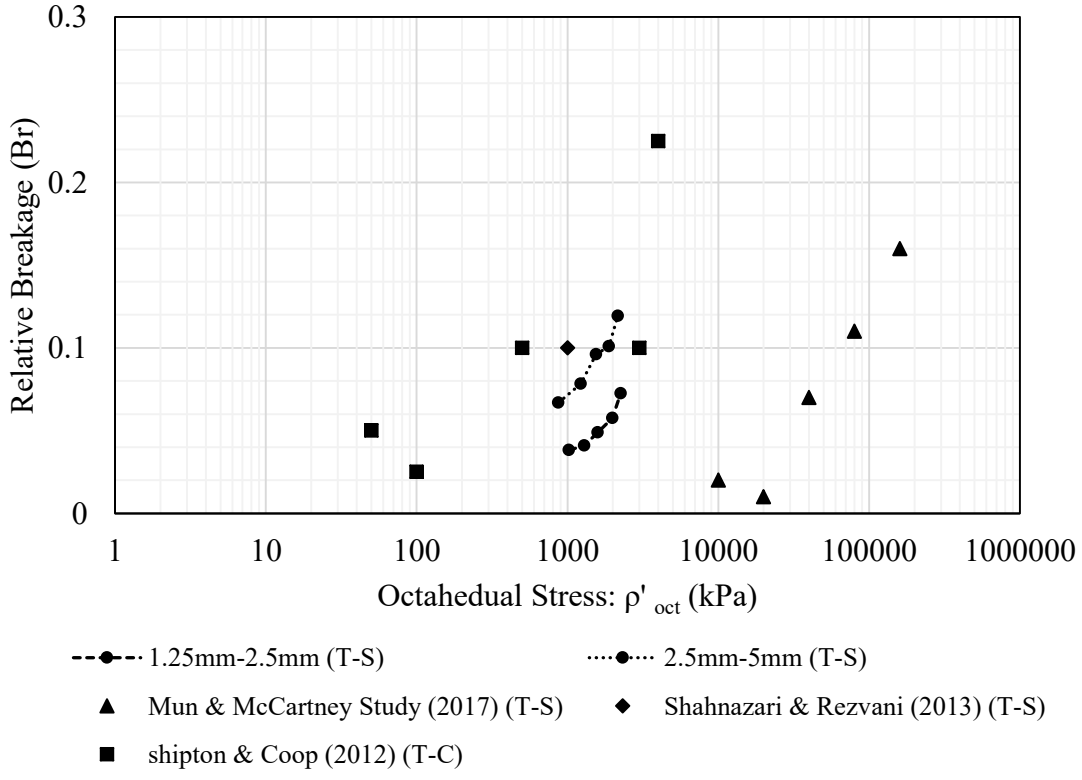

Figure 29. Comparison of Br values in this study to those found in the literature

Implication for Qualitative Manufacturing of ACT Aggregates

There are several practical implications from this work related to ACT aggregate manufacturing. Firstly, it is apparent that similar to other particle breakage studies in the literature, larger particle sizes (i.e. 5mm-2.5mm size fraction in this study) are more susceptible to the particle breakage relative to smaller size particles. This suggests that if ACT aggregates in this study were to be used in geotechnical applications in which they will be subjected to shear and/or compression conditions where the mean stresses approached or exceeded those in this research, aggregates in the 2.5mm-1.25mm size range would perform better than those in the 5 mm-2.5 mm range. Given that the particle sizes can be controlled in the aggregate manufacturing process, a move to smaller particles may be preferred in geotechnical applications, especially those in shear applications (i.e. roadways, embankment slopes). If the aggregate is to be used in applications where shear is limited and loading is predominately isotropic (or near), then the amount of particle breakage is expected to be small (e.g. wide fills). For example, for the 2.5mm-1.25mm size, Br values were less than 0.01 for mean stresses up to 1400 kPa in triaxial compression tests. This stress range would be above most common stress applications for urban developments.

Exposure to Freeze-Thaw Cycling

As shown Figure 28, for freeze-thaw cycle tests carried out to only 20 cycles, resulted in relative breakage that was at or near that from the triaxial shear tests for the 2.5mm-1.25mm ACT aggregate. This suggests that care should be taken to ensure exposure to freeze thaw cycles are limited for this size of aggregate. However, the freeze-thaw performance of the 2.5mm-1.25mm size was significantly better than that of the 5mm-2.5mm size. For the 20 f/t cycles, limited breakage was observed. This observation

should be taken within the context that 20 f/t cycles may not be representative of field applications (i.e. more f/t cycles may be present in the field). This is an area that further testing would be useful. The manufacturing of ACT aggregates in the 2.5 mm and less size appear to be desirable at this stage. It also may be preferable at this juncture to limit ACT aggregate exposure to f/t cycles until this work can be completed. This recommendation is in the context of geotechnical applications in which the ACT aggregate would be exposed to f/t testing.

4.6 Summary and Conclusions

This chapter has presented the results of various tests designed to examine the amount of particle breakage that occurs for the CKD derived ACT aggregate developed in this study. Of particular emphasis in this study is the role of particle size on relative breakage (B_r) for the ACT aggregate. Triaxial compression, triaxial shear and freeze/thaw cycling tests were performed on the ACT aggregate using the entire grain size distribution and with isolated particle sizes (5mm-2.5mm and 2.5mm-1.25mm) to assess particle breakage. The grain sizes before and after testing were used to calculate the relative breakage, B_r. This parameter, albeit not without its problems, does provide a fairly simple technique to provide relative comparison between grain sizes and also allows comparisons to be made with previous studies related to calcareous sands and other more durable sands.

It was shown in this study that similar to other studies in the literature for natural soils, the majority of particle breakage in the ACT aggregate occurred in the large particle

size (5mm-2.5mm) relative to the smaller particle size (2.5mm-1.25mm). This observation was present regardless of the test method performed.

Particle breakage results from freeze-thaw testing showed that for the entire sample and 5mm-2.5 mm size corresponded to similar or slightly less particle breakage as that under triaxial shear. This suggests that environmental factors such as freeze-thaw may be as important a consideration in application to loading conditions. In contrast, the particle breakage of the 2.5mm-1.25mm aggregate after 20 cycles of freeze-thaw was small and similar in magnitude to the same size aggregate under low to medium confining pressures.

The performance of the ACT aggregate in terms of relative breakage (i.e. B_r) was similar or slightly better than natural calcareous sand results found in the literature but substantially higher than more durable mineral fraction sands. This is an interesting finding in that calcareous sands, although not the most desirable sand to use in construction, can be used when its geotechnical limits are known and loads and strains are limited to account for this performance. More work is required to examine these limited conditions for the ACT aggregate, especially at higher strain levels and higher levels of freeze-thaw performance.

Chapter 5: Conclusion

5.1 Summary and Conclusion

As noted in Chapter 1, the objectives of this thesis were to:

1) Provide a literature review related to topics in this thesis (i.e. ACT literature review, ACT aggregate pelleting process, CKD, aggregate strength and durability, etc.)

2) Perform the ACT aggregate pelleting process in Dalhousie laboratories and assess the physical and chemical properties of the resulting aggregates developed from the CKD material studied.

3) Assess the durability of the resulting aggregate under different loading conditions (i.e. physical durability) and freeze-thaw (F/W) (i.e. environmental durability) using commonly employed durability assessment techniques. Further, to assess the role of particle size on the observed durability of the manufactured aggregate studied in this thesis.

The results of the literature review can found in Chapter 2 and will not be summarized here.

To assess the geotechnical and geo-environmental properties of carbonated aggregate made from CKD, several performance tests were performed. The sand product was shown to have a mature individual aggregate strength of more than 1 MPa and, upon compaction, a friction angle of 39° when subjected to drain triaxial testing under confining pressures ranging from 100 to 250 kPa. The aggregate displayed a very high durability to wet–dry cycling using the slake durability test and no noticeable changes in grain size when subjected to an isotropic confining compression test. Freeze–thaw

cycling at −17·5 ± 2·5°C for 20 cycles showed a reduction in grain size that warranted further investigation and future improvement. One-point batch adsorption showed that the ACT aggregate removed 90% of the selected heavy metals from prepared solutions, indicating potential for geo-environmental applications such as permeable reactive barriers.

Chapter 4 involved minor modification of the aggregate manufacturing process and additional testing to examine the durability (i.e. particle breakage) of the CKD derived aggregate. The role of particle size on relative breakage (B_r) for the ACT aggregate was also examined in this chapter. Triaxial compression, triaxial shear and freeze/thaw cycling tests were performed on the ACT aggregate using the entire grain size distribution and with isolated particle sizes (5mm-2.5mm and 2.5mm-1.25mm) to assess particle breakage. The grain sizes before and after testing were used to calculate the relative breakage, B_r. This parameter provided a simple technique for relative comparison between grain sizes and also allowed comparisons to be made with previous studies related to calcareous sands and other more durable sands. It was shown that the majority of particle breakage in the ACT aggregate occurred in the large particle size (5mm-2.5mm) relative to the smaller particle size (2.5mm-1.25mm). This observation was present regardless of the test method performed (i.e. triaxial compression or triaxial shear). Particle breakage results from freeze-thaw testing showed that for the entire sample and 5mm-2.5 mm size corresponded to similar or slightly less particle breakage as that under triaxial shear suggesting that environmental factors such as freeze-thaw may be as important a consideration in application to loading conditions. In contrast, the particle breakage of the 2.5mm-1.25mm aggregate

after 20 cycles of freeze-thaw was small and similar in magnitude to the same size aggregate under low to medium confining pressures. The performance of the ACT aggregate in terms of relative breakage (i.e. B_r) was similar or slightly better than natural calcareous sand results found in the literature but substantially higher than more durable mineral fraction sands. This is an interesting finding in that calcareous sands, although not the most desirable sand to use in construction, can be used when its geotechnical limits are known and loads and strains are limited to account for this performance. More work is required to examine these limited conditions for the ACT aggregate, especially at higher strain levels and higher levels of freeze-thaw performance.

5.2 Recommendations for Future Research

The work in this thesis has examined, for the first time to the author's knowledge, the role of particle breakage in a manufactured CKD ACT aggregate under different mechanical and environmental loading conditions. While this work provides a good initial starting point for this topic, additional research should and can be performed. The following are ideas for future research:

1) Examine the potential for improvements in the manufacturing process to improve the durability of the ACT aggregate in this study. Methods to assess the particle breakage used in this thesis can be used.

2) Examined the critical state performance of the aggregate under higher strain rates using the methods described by Coop (1990) to assess the particle breakage at critical state conditions.

3) Compare laboratory aggregates to full scale plant aggregates in terms of particle breakage.

4) Examine the potential blending of aggregates with strategic grain sizes of more durable particles to improve upon the breakage of entire grain distribution of the ACT aggregate.

5) Examine modifications to the manufacturing process to develop sand sizes in the 0.5 mm to 1 mm range to see if improvements in particle durability can be obtained.

Bibliography

Adaska, S. W., & Taubert, H. D. (2008). Beneficial uses of cement kiln dust. *2008 IEEE/PCA 50th Cement Industry Technical Conference*, Miami, FL, USA. 210–228, Retrieved from http://dx.doi.org/10.1016/j.jclepro.2015.09.111

Alberta Government (2015). Quantification Protocol for CO_2 Capture and Permanent Storage in Deep Saline Aquifers. *Alberta Environment and Parks.* Edmonton, Alberta, CA, ISBN: 978-0-7785-7221-3

Al-Harthy, A.S., Taha, R., & Al-Maamary, F. (2003). Effect of cement kiln dust (CKD) on mortar and concrete mixtures. *Construction and Building Materials*. 17(5), 353–360.

Altuhafi, F. N., & Coop, M. R. (2011). Changes to particle characteristics associated with the compression of sands, *Geotechnique* 61(6), 459–471. doi: 10.1680/geot.9.P.114

Arandigoyen, M., Bicer-Simsir, B., Alvarez, J. I., & Lange, D. A. (2006). Variation of microstructure with carbonation in lime and blended pastes. *Journal of Applied Surface Science*, 252(20), 7562–7571. Retrieved from http://dx.doi.org/10.1016/j.apsusc.2005.09.007

Arslan, H., & Baykal, G. (2006). Analyzing the crushing of granular materials by sound analysis technique. *Journal of Testing and Evaluation*, 34(6): 1–7, Retrieved from https://doi.org/10.1520/JTE100032

Asha, S., & Maria, C. S. (2006). Development of Criteria for the Utilization of Cement Kiln Dust (CKD) in Highway Infrastructures. *Report Federal Highway Administration (FHWA)/Joint Transportation Research Program (JTRP) 2005/10*. Purdue University, West Lafayette, IN, USA, Retrieved from https://doi.org/10.5703/1288284313395

Assen, N., Jung, J., & Bardow, A. (2013). Life-cycle assessment of carbon dioxide capture and utilization: avoiding the pitfalls. *Energy Environmental Science*. 6, 2721-2734.

ASTM D 2434-68. (2006). Standard test method for permeability of granular soils (constant head). *ASTM International*, West Conshohocken, PA, USA.

ASTM D 4644-08. (2008). Standard test method for slake durability of shales and similar weak rocks. *ASTM International*, West Conshohocken, PA, USA.

ASTM C 1733-10. (2010). Standard test methods for distribution coefficients of inorganic species by the batch method. *ASTM International*, West Conshohocken, PA, USA.

ASTM D 4179-11. (2011a). Standard test method for single pellet crush strength of formed catalysts and catalyst carriers. *ASTM International*, West Conshohocken, PA, USA.

ASTM D7181. (2011b). Standard test method for consolidated drained triaxial compression test for soils. ASTM International, *West Conshohocken*, PA, USA.

ASTM D2487. (2011c). Standard test method for classification of soil for engineering purposes (Unified Soil Classification System). *ASTM International*, West Conshohocken, PA, USA.

Barnard, L. H., Boardman, D. I., Rogers, C. D., Hills, C. D., Carey, P. J., Canning, K., & Macleod, C. L. (2005). Influence of Soil and Binder Properties on the Efficacy of Accelerated Carbonation. *STARNET Conference.* University of Cambridge. 285-295. Retrieved from DOI: 10.1201/9781439833933.ch36

Bauer, M., Gassen, M., Stanjek, H., & Peiffer, S. (2011). Carbonation of lignite fly ash at ambient T and P in a semi-dry reaction system for CO_2 sequestration. *Applied Geochemistry*. 26, 1502-1512.

Beruto, D. T., Barberis, F., & Botter, R. (2005). Calcium carbonate binding mechanisms in the setting of calcium and calcium-magnesium putty-limes. *Journal of Cultural Heritage,* 6**,** 253-260.

Bhatty, J. I., Bhattacharja, S., & Todres, H. A. (1996). Use of Cement Kiln Dust in Stabilizing Clay Soils. *Portland Cement Association*, Skokie, IL, USA, Portland Cement Association R&D Serial No. 2035.

Bleys, G. (2016), Technology watch: Carbon Dioxide Conversion. Retrieved from http://www.essenscia.be/en/Document/Download/16288

BSI BS EN 13055-4. (2016). Lightweight aggregates. *BSI (British Standards Institution)*, London, UK. Carbon8 (2016). Retrieved from http://c8a.co.uk/ (accessed 10/03/2016)

BSI BS EN 12457-4. (2002). Characterisation of waste. Leaching Compliance test for leaching of granular waste materials and sludges. British Standard Institution (BSI), London, UK.

Carbon8. (2016). Retrieved from http://c8a.co.uk/

CIWM (Chartered Institution of Wastes Management). (2014). Grundon Invests Further Millions in Carbon8 Aggregates. *Certified International Wealth Manger (CIWM)*. Northampton, UK. Retrieved from http://www.ciwm.co.uk/

Coop, M. (1990). The mechanics of uncemented carbonate sands. *Geotechnique,* 40 (4), 607–615.

Cooper, C., & Phillips, C. (2009). A Technical Basis for Carbon Dioxide Storage, *Science Direct, Energy Procedia,* 1(1), 1727-1733. Retrieved from https://doi.org/10.1016/j.egypro.2009.01.226

Costa, I., Baciocchi, R., Polettini, A., Pomi, R., Hills, C.D., & Carey, P.J. (2007). Current status and perspectives of accelerated carbonation processes on municipal waste combustion residues. *Environmental Monitoring and Assessment*, 135, 55-75.

Costa, G., Baciocchi, R., Polettini, A., Pomi, R., Hills, C. D., & Carey, P. J. (2007). Current status and perspectives of accelerated carbonation processes on municipal waste combustion residues. *Environmental Monitoring Assessment,* 135(1), 55–75. Retrieved from http://dx. doi.org/10.1007/s10661-007-9704-4

Cultrone, G., Sebastian, E., & Huertas, M. O. (2005). Forced and natural carbonation of lime-based mortars with and without additives: Mineralogical and textural changes. *Cement and Concrete Research,* 35**,** 2278-2289.

CSI (Cement Sustainability Initiative). (2016). World Business Council for Sustainable Development. *CSI*, Geneva, Switzerland. Retrieved from http://www.wbcsdcement.org/

De Bono, J. P., & McDowell, G. R. (2014). DEM of triaxial tests on crushable sand. *Granular Matter,* 16(4), 563–572. Retrieved from https://doi.org/10.1007/s10035-014-0502-8

Domingo. C., Loste, E., Gomez-Morales, J., Garcia-Carmona, J., & Fraile, J. (2006). Calcite precipitation by a high-pressure CO_2 carbonation route. *Journal of Supercritical Fluids,* 36(3), 202–215. Retrieved from http://dx.doi. org/10.1016/j.supflu.2005.06.006

Edward, S. R., Davison, J.E., & Herzog, H.J. (2015). The cost of CO_2 capture and storage, *International Journal of Greenhouse Gas Control*. 40, 378-400.

Edwards, L. M. (2006). The effect of alternate freezing and thawing on aggregate stability and aggregate size distribution of some Prince Edward Island soils. *Journal of Soil Science,* 42(2), 193–204. Retrieved from http://dx.doi.org/10.1111/j.1365-2389.1991.tb00401.x

Einav, I. (2007). Breakage mechanics-Part 1: theory. *Journal of the Mechanics and Physics of Solids*. 55(6), 1274–1297.

El-Aleem, S.A., Abd-El-Aziz, M.A., Heikal, M., & El-Didamony, H. (2005). Effect of Cement Kiln Dust Substitution on Chemical and Physical Properties and Compressive Strength of Portland and Slag Cements. *The Arabian Jounal for Science and Engineering.* 30, 263-273.

Fernández, B. M., Simons, S. J. R., Hills, C. D., & Carey, P. J. (2004a). A review of accelerated carbonation technology in the treatment of cement-based materials and sequestration of CO_2. *Journal of Hazardous Materials,* 112(3), 193–205. Retrieved from http://dx.doi.org/10.1016/j.jhazmat.2004.04.019

Fernández, B. M., Li, X., Simons, S. J. R., Hills, C. D., & Carey, P. J. (2004b). Investigation of Accelerated Carbonation for the Stabilization of MSW Incinerator Ashes and the Sequestration of CO_2. *Green Chemistry,* 6, 428-436.

Francesca, C., & Giulia, M. B. V. (2013). Breakage of an artificial crushable material under loading. *Granular Matter,* 15(5), 661-673 DOI 10.1007/s10035-013-0432-x

Freedonia Group (2013). *Industry Study 3078: World Construction Aggregates*. Freedonia Group. Cleveland, OH, USA.

Gamble, J. C. (1971). *Durability–Plasticity Classification and Shales and Other Argillaceous Rocks. PhD thesis*, University of Illinois at Urbana-Champaign, Champaign, IL, USA.

Gunning, P. J. (2011). *Accelerated Carbonation of Hazardous Wastes*. PhD thesis, University of Greenwich, London, UK.

Gunning, P. J., Hills, C. D., & Carey, P. J. (2009). Production of lightweight aggregate from industrial waste and carbon dioxide. *Waste Management*, 29(10), 2722–2728. Retrieved from http://dx.doi.org/10.1016/j.wasman.2009.05.021

Gunturi, M., Ravichandran, P. T., Annadurai, R., & Divya, K. K. (2014). Study on Strength Characteristics of Soil Using Soil Stabilizer RBI – 81. *International Journal of Research in Engineering and Technology*. 03, 201-204.

Hardin, B.O. (1985). Crushing of soil particles. *Journal of Geotechnical Engineering,* 111 (10), 1177–1192.

Hossain, K. M. A. (2011). Stabilized Soils Incorporating Combinations of Rice Husk Ash and Cement Kiln Dust. *Journal of Materials in Civil Engineering*, 23, 1320-1327.

Huang, J. T., & Airey, D. W. (1998). Properties of artificially cemented carbonate sands. *Journal of Geotechnical and Geoenvironmental Engineering,* 124**,** 482-498.

Huijgen, W. J., & Comans, R. N. J. (2005a). Carbon Dioxide Sequestration by Mineral Carbonation: Literature Review Update 2003–2004. *Energy Research Centre of the Netherlands*, Petten, the Netherlands. Report ECN-C-05-022.

Huijgen, W.J., & Comans, R.N.J. (2005b). Mineral CO_2 sequestration by carbonation of industrial residues. Literature overview and selection of residue. *Energy Research Centre of the Netherlands, Petten, The Netherlands*. ECN-C-05-074 Retrieved from https://www.ecn.nl/docs/library/report/2005/c05074.pdf

Huntzinger, D. N., Gierke, J. S., Sutter, L. L., Kawatra, S. K., & Eisele, T. C. (2009). Mineral carbonation for carbon sequestration in cement kiln dust from waste piles. *Journal of Hazardous Materials*, 168, 31–37.

Indraratna, B., Lackenby, J., & Christie, D. (2005). Effect of Confining Pressure on the Degradation of Ballast under Cyclic Loading, *Geotechnique, Institution of Civil Engineers*, 55(4), 325-328.

Jain, P. & Goliya, H. S. (2014). Chemical Stabilization of Black Cotton Soil for Sub-Grade Layer. *International Journal of Structural and Civil Engineering Research*. 03, 160-166

Johnson, D. C., Macleod, C. L., & Hills, C. D. (2003). Accelerated Carbonation of Stainless Steel Slag. *Waste Materials in Construction: Progress on the way to sustainability,* 24(6), 671-8 doi: 10.1080/09593330309385602

Kent. A, & Bhavna, S. (2016). *Nonconventional and Vernacular Construction Materials (Characterisation, properties and Applications)*. UK: Woodhead publishing

Khan, M. I., & Lynsdale, C. J. (2002). Strength, permeability, and carbonation of high-performance concrete. *Cement and Concrete Research,* 32**,** 123-131.

Khunthongkeaw, J., Tangtermsirikul, S., & Leelawat, T. (2006). A study on carbonation depth prediction for fly ash concrete. *Construction and Building Materials,* 20**,** 744-753.

Klotz, E. U., & Coop, M. R. (2001). An investigation of the effect of soil state on the capacity of driven piles in sands. *Geotechnique,* 51(9), 733-751.

Konrad, J. M., & Salami, Y. (2017). Particle breakage in granular materials a conceptual framework. *Canadian Geotechnical Journal,* Retrieved from https://doi.org/10.1139/cgj-2017-0224

Lackner, K.S., Butt, D.P., & Wendt, C.H. (1997). Progress on binding CO_2 in mineral substrates. *Energy Convers Management.* 38, 259 - 264. DOI: 10.1016/S0196-8904(96)00279-8

Lade, P.V., Yamamuro, J.A., & Bopp, P.A. (1996). Significance of particle crushing in granular materials. *Journal Geotechnical. Engineering American Society of Civil Engineers (ASCE),* 122(4), 309–316.

Lambe, T. W., & Whitman, R. V. (1969). *Soil Mechanics* (pp. 423-455). New York, NY, USA: John Wiley & Sons, Inc.

Lee, K. L., & Farhoomand, I. (1967). Compressibility and crushing of granular soil. *Canadian Geotechnical Journal*, 4(1), 68–86. Retrieved from http://dx.doi.org/10.1139/t67-012

Li, Y., Wu, D., Zhang, J., Chang, L., Wu, D., Fang, Z., & Shi, Y. (2000). Measurement and statistics of single pellet mechanical strength of differently shaped catalysts. *Powder Technology,* 113(1–2), 176–184, Retrieved from https://doi.org/10.1016/S0032-5910(00)00231-X

Liu, L., Ha, J., Hashida, T., & Teramura, S. (2001). Development of a CO_2 solidification method for recycling autoclaved lightweight concrete waste. *Journal of Material Science Letters,* 26**,** 1791-1794.

Li, L., Zhao, N., Wei, W., & Sun, Y. (2013). Random lasing from dye-doped chiral nematic liquid crystals in oriented and non-oriented cells. *The European Physical Journal B*. 86, 112-130.

Lobo-Guerrero, S., & Vallejo, L. E. (2005). Crushing of weak granular material: Experimental-numerical analyses. *Geotechnique*, 55(3), 245–249. Retrieved from https://doi.org/10.1680/geot.2005.55.3.245

Luzzani, L., & Coop, M.R. (2002). On the relationship between particle breakage and the critical state of sands. *Soils Found*. 42(2), 71–82.

Mackie, A., Boilard, S., Walsh, M. E., & Lake, C. B. (2010). Physicochemical characterization of cement kiln dust for potential reuse in acidic wastewater treatment. Journal of Hazardous Materials 173(1–3), 283–291, http://dx.doi.org/10.1016/j.jhazmat.2009.08.081

Markewitz, P., Kuckshinrichs, W., Leitner, W., Linssen, J., Zapp, P., & Bongartz, R. (2012). Worldwide Innovations in the Development of Carbon Capture Technologies and the Utilization of CO_2. *Energy Environment Science.* 5, 7281-7305.

Maries, A., Hills, C. D., Whitehead, K. & Macleod, C. L. (2001). Enhanced cement stabilization of contaminated clay soils. *Problematic soils,* Retrieved from https://www.icevirtuallibrary.com/doi/abs/10.1680/ps.30435.0013

Marsal, R. J. (1967). Large-scale testing of rockfills materials. J. Soil Mech. Found. Engineering Division. *American Society of Civil Engineers (ASCE),* 93(2), 27–44.

Maslehuddin, M., Al-Moudi, O. S. B., Shameem, M., Rehman, M. K., & Ibrahim, M. (2008). Usage of cement kiln dust in cement products – research review and preliminary investigation. *Construct Build Material*. 22, 2369-2375.

Meylan, F. D., Moreau, V., & Erkman, S. (2015). CO_2 utilization in the perspective of industrial ecology, an overview. *Journal of CO_2 Utilization,* 12, 101-108.

Mindess, S., Young, J. F., & Darwin, D. (2003). *Concrete (Second Edition)* (pp. 121-134). Upper Saddle River, NJ, USA: Pearson Education, Inc.

Miura, N., & O-Hara, S. (1979). Particle-crushing of a decomposed granite soil under shear stresses. *Soils and Foundations*, 19(3), l–14. doi:10.3208/sandf1972. 19.3_1

Molenaar, N., & Venmans, A. A. M. (1993). Calcium carbonate cementation of sand: A method for producing artificially cemented samples for geotechnical testing and a comparison with natural cementation processes. *Engineering Geology,* 35**,** 103-122.

Mun, M., & Cho, H. (2013). Mineral carbonation for carbon sequestration with industrial waste. *Energy Procedia*. 37, 6999-7005.

Mun, W., & McCartney, J. S. (2017). Effective Stress Analysis of the Undrained Compression of Unsaturated Soils, *19th International Conference on Soil Mechanics and Geotechnical Engineering.* Seoul.

Nova Scotia Environment (NSE). (2014). *Environmental Quality Standards for Contaminated Sites – Rationale and Guidance Document.*

Nova Scotia Department of Transportation and Infrastructure Renewal (NSTIR). (2014). *Annual Accountability Report for the Fiscal year*.

O'connor, W. K., Dahlin, D. C., Rush, G. E., Gerdemann, S. J., Penner, L. R., & Nilsen, D. N. (2005). Final Report Aqueous Mineral Carbonation: Mineral Availability, Pretreatment, Reaction Parametrics. And Process Studies. *Office of Process Development National Energy Technology Laboratory, Office of Fossil Energy, US Department Of Energy*, DOE/ARC-TR-04-002.

Ovalle, C., Dano, C., Hicher, P. Y., & Cisternas, M. (2015). Experimental framework for evaluating the mechanical behavior of dry and wet crushable granular materials based on the particle breakage ratio, *Canadian Geotechnical Journal*, 52, 587–598. doi.org/10.1139/cgj-2014-0079

PCA (Portland Cement Association). (2011). Report on Sustainable Manufacturing. *PCA*, Skokie, IL, USA. Retrieved from http://www.cement.org/

Rafat, S. (2006). Utilization of cement kiln dust (CKD) in cement mortar and concrete an overview. *Conservation and Recycling*, 315-338.

Rendek, E., Ducom, G., & Germain, P. (2006). Influence of organic matter on municipal solid waste incinerator bottom ash carbonation. *Chemosphere*. 64(7), 1212–1218.

Roy, S. K., Poh, K. B. & Northwood, D. O. (1999). Durability of concrete--accelerated carbonation and weathering studies. *Building and Environment,* 34**,** 597-606.

Russell, D., Basheer, P. A. M., Rankin, G. I. B., & Long, A. E. (2001). Effect of relative humidity and air permeability on prediction of the rate of carbonation of concrete. *Proceedings of the Institution of Civil Engineers, Structures and Buildings,* 146**,** 319-326.

Richardson, D. N. (2009). Quick Test for Durability Factor Estimation. Missouri University of Science and Technology, Rolla, MO, USA, Report 0R09.020, 24–30.

Sanna, A., Uibu, M., Caramanna, G., Kuusik, R., & Maroto, M.M. (2014). A review of mineral carbonation technologies to sequester CO_2. *Chemical Society Reviews.* 43, 8049-8080.

SCOT. (2015). A Vision for Smart CO_2 Transformation in Europe (Using CO_2 as a resource), *Smart CO_2 Transformation*. Retrieved from http://www.scotproject.org/images/SCOT%20Vision.pdf

SETIS (Strategic Energy Technologies Information System). (2016). Carbon Capture Utilization and Storage. *European Commission.* Retrieved from https://setis.ec.europa.eu/setis-reports/setis-magazine/carbon-capture-utilisation-and-storage

Shahnazari, H., & Rezvani, R. (2013). Effective parameters for the particle breakage of calcareous sands: An experimental study. *Engineering Geology*, 159, 98-105. Retrieved from http://dx.doi.org/10.1016/j.enggeo.2013.03.005

Shipton, B., & Coop, M. R. (2012). On the compression behaviour of reconstituted soils, *Soil and Foundation*. 52(4), 668-681. Retrieved from https://doi.org/10.1016/j.sandf.2012.07.008

Simms, P. H., & Yanful, E. K. (2004). A discussion of the application of mercury intrusion porosimetry for the investigation of soils, including an evaluation of its use to estimate volume change in compacted clayey soils. *Geotechnique* 54(6), 421–426, Retrieved from http://dx.doi.org/10.1680/ geot.2004.54.6.421.

Sreekrishnavilasam, A., King, S., & Santagata, M. (2006). Characterization of fresh and landfilled cement kiln dust for reuse in construction applications. *Engineering Geology*. 85, 165.

Styring, P., Jansen, D., Coninck, De. H., Reith, H., & Armstrong, K. (2011). Carbon Capture and Utilization in the Green Economy. *Centre for Low Carbon Futures*. 501, ISBN: 978-0-9572588-1-5.

Uibu, M., & Kuusik, R. (2009). Mineral Trapping of CO_2 via Oil Shale Ash Aqueous Carbonation: Controlling Mechanism of Process Rate and Development of Continuous-Flow Reactor System. *Oil Shale*, *26*, 40-58.

Uliasz-Bochenczyk, A. (2011). Mineral Sequestration of CO_2 Using Water Suspensions of Selected Fly Ashes from the Combustion of Lignite Coal. *Gospodarka Surowcami Mineralnymi-Mineral Resources Management.* 27, 145-154.

Uliasz-Bochenczyk, A., Gawlicki, M., & Pomykala, R. (2012). Evaluation of the possibilities of sequestration of carbon dioxide in aqueous suspensions of selected fly ash. *Gospodarka Surowcami Mineralnymi-Mineral Resources Management.* 28, 103-112.

University of Greenwich. (2012). University's 'green' invention to treat waste materials goes into commercial production. Retrieved from http://www2.gre.ac.uk/about/news/articles/2012/a2182-carbon-8

Upma, J., & Kumar, S. (2015). Effect of Cement Kiln Dust and Chemical Additive on Expansive Soil at Subgrade Level, *International Journal of Innovative Research in Science, Engineering and Technology.* 4, 3759-3767.

Van Ginneken, L., Dutré, V., Adriansens, W., & Weyten, H. (2004). Effect of liquid and supercritical carbon dioxide treatments on the leaching performance of a cement-stabilised waste form. *Journal of Supercritical Fluids,* 30**,** 175-188.

Venhuis, M., & Reardon, E. J. (2003). Carbonation of cementitious waste forms under supercritical and high pressure subcritical conditions. *Environmental Technology,* 24**,** 877-887.

Valsangkar, A. J., & Holm, T. A. (1999). Mechanical durability of expanded shale lightweight aggregate. *Geotechnical Testing Journal*, 22(4), 329–333. Retrieved from https://doi.org/10.1520/GTJ11246J.

Washburn, E. W. (1921). Note on a method of determining the distribution of pore sizes in a porous material. *Proceedings of the National Academy of Sciences of the United States of America,* 7(4), 115–116.

Young, J. F., Berger, R. L., & Breese, J. (1974). Accelerated curing of compacted calcium silicate mortars on exposure to CO_2. *Journal of the American Ceramic Society,* 57**,** 394-397.

Yamamuro, J. A., & Lade, P. V. (1993). Effects of strain rate on instability of granular soils. *Geotechnical Testing Journal*, 16(3), 304–313.

Zapp, P., Schreiber, A., Marx, J., Haines, M., Hake, J. F., & Gale, J. (2012). Overall Environmental Impacts of CCS Technologies – A Life Cycle Approach. *Internal Journal of Greenhouse Gas Control*. 8, 12-21.

Zhang, X., Wu, K., & Yan, A. (2004). Carbonation property of hardened binder pastes containing super-pulverised blast furnace slag. *Cement and Concrete Composites,* 26**,** 371-374.

Zheng, W., & Tannant, D. (2016). Frac sand crushing characteristics and morphology changes under high compressive stress and implications for sand pack permeability. *Canadian Geotechnical Journal* 53(9), 1412-1423. Retrieved from https://doi.org/10.1139/cgj-2016-0045

Zheghal, M. (2009). The impact of grain crushing on road performance. *Geotechnical and Geological Engineering*. 27, 549–558.

Appendix A. Detection limits of Varian Vista MPX CCD ICP-OES Instruments

Element	Detection limit (ug/L)	
	Axial	Radial
Ag	0.50	1.00
Al	0.90	4.00
As	3.00	12.00
As	4.00	11.00
Ba	0.03	0.15
Be	0.05	0.15
Ca	0.01	0.30
Cd	0.20	0.50
Co	0.40	1.20
Cr	0.50	1.00
Cu	0.90	1.50
Fe	0.30	0.90
K	0.30	4.00
Li	0.06	1.00
Mg	0.05	0.10
Mn	0.10	0.13
Mo	0.50	2.00
Na	0.20	1.50
Ni	0.70	2.10
P	4.00	25.00
Pb	1.50	8.00
Rb	1.00	5.00
S	4.00	13.00
Sb	3.00	16.00
Se	4.00	16.00
Sr	0.02	0.10
Sn	2.00	8.00
Ti	0.50	1.00
Tl	2.00	13.00
V	0.70	2.00
Zn	0.20	0.80

Appendix B. Entire ACT aggregate Particle Assemblage Shear Resistance

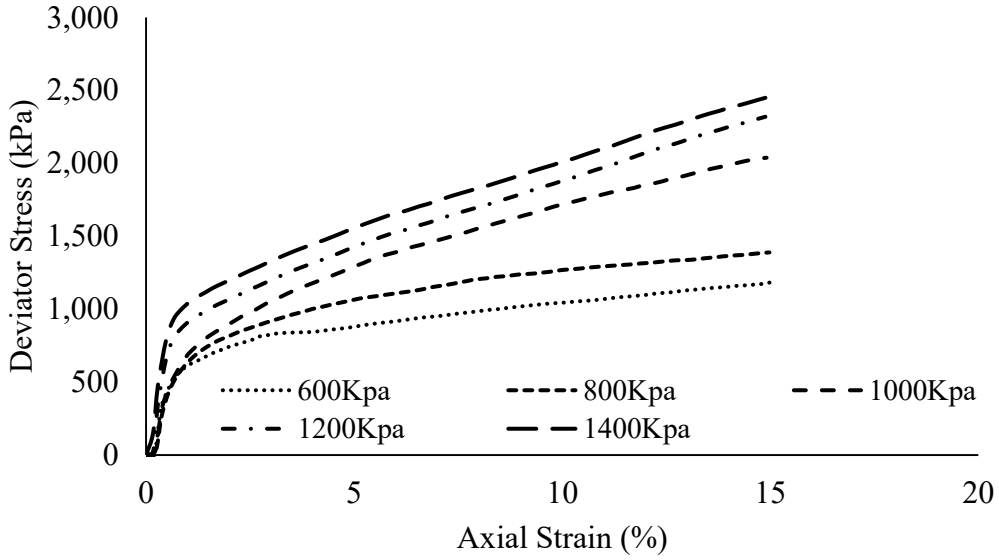

A. Stress–strain curves for triaxial testing (Entire size ACT Aggregate)

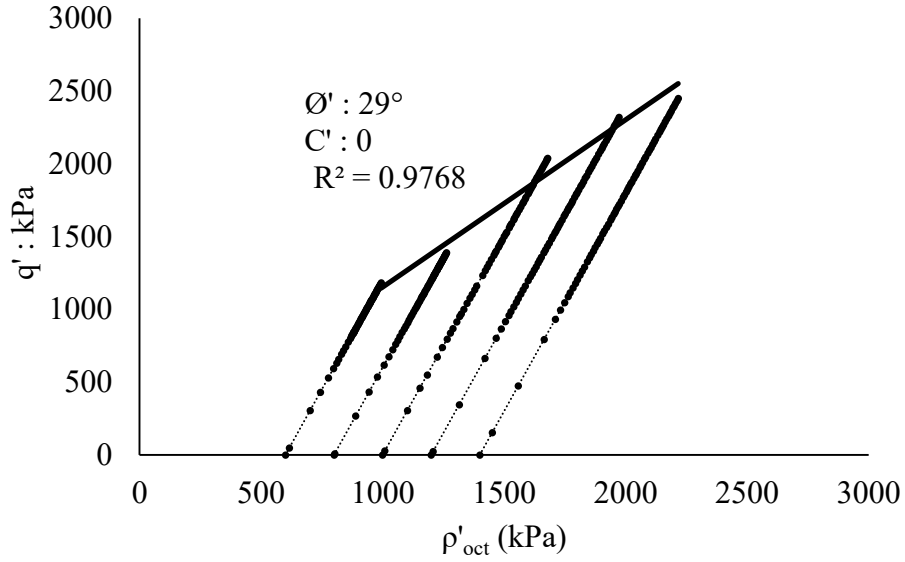

B. Failure envelope for ACT aggregate from CKD triaxial testing (Entire size ACT aggregate)

Appendix C. 2.5-5mm ACT aggregate Particle Assemblage Shear Resistance

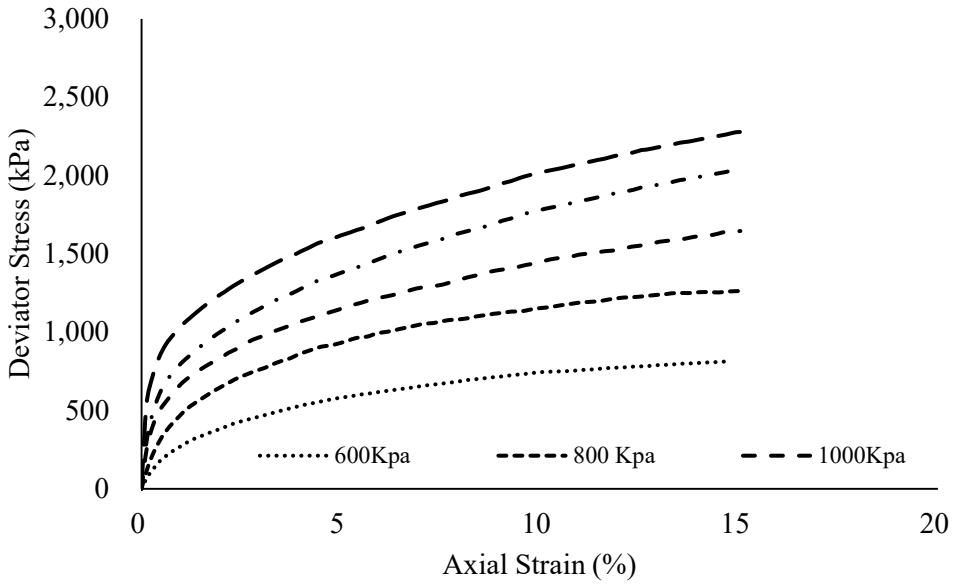

A. Stress–strain curves for triaxial testing (2.5-5 mm size ACT Aggregate)

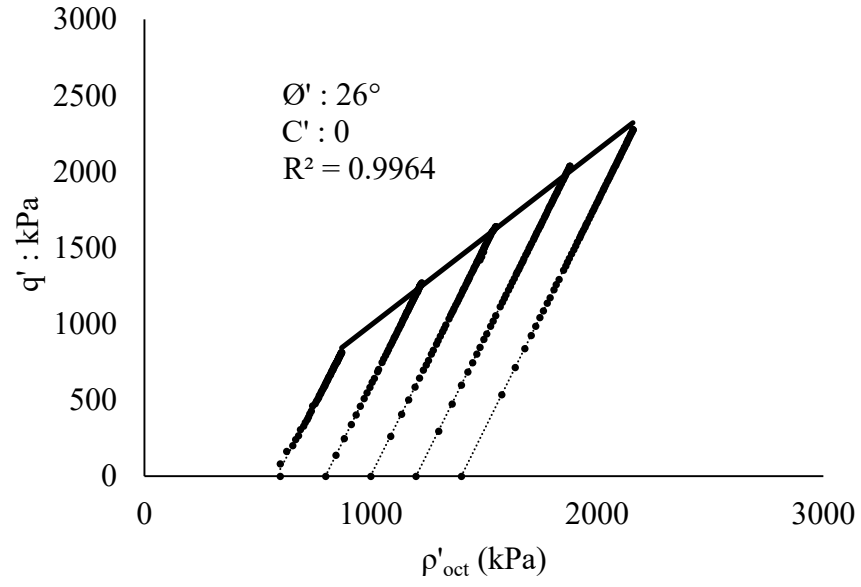

B. Failure envelope for ACT aggregate from CKD triaxial testing (2.5-5mm size ACT aggregate)

Appendix D. 1.25-2.5 mm ACT aggregate Particle Assemblage Shear Resistance

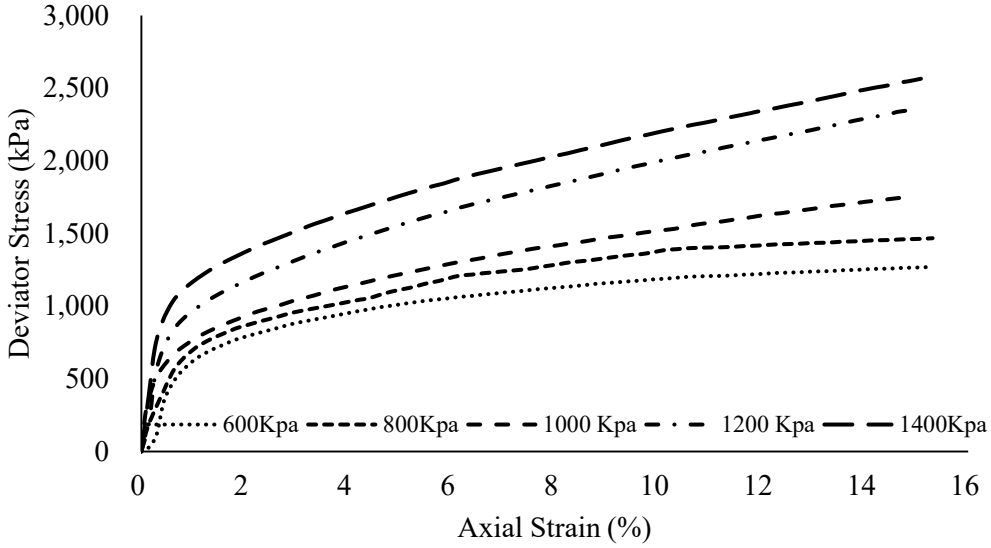

A. Stress–strain curves for triaxial testing (1.25-5 mm size ACT Aggregate)

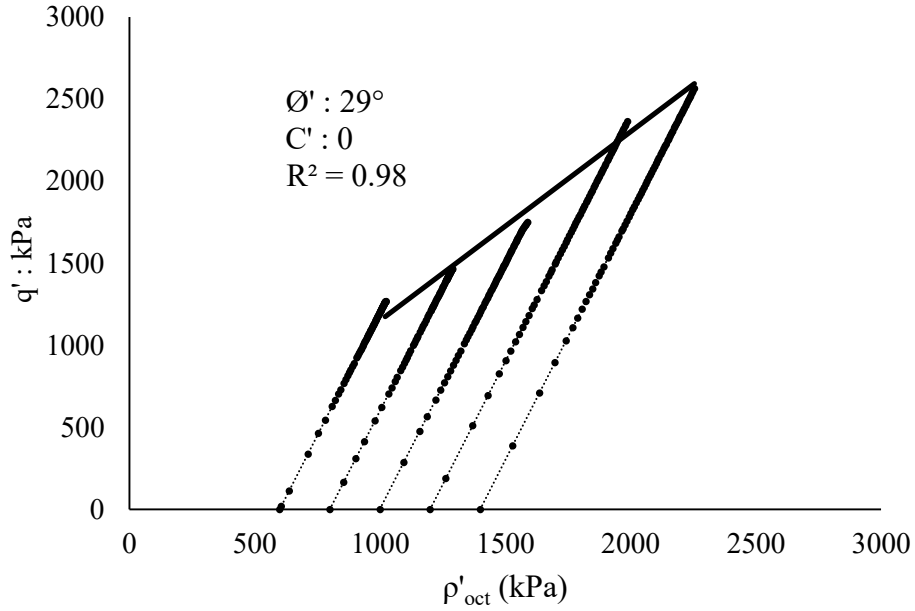

B. Failure envelope for ACT aggregate from CKD triaxial testing (1.25-2.5mm ACT aggregate)

Appendix E. Copyright Permission Letter

March 26, 2018

Environmental Geotechnics
ICE Publishing
8 Storey's Gate
London SWIP 3AT, UK

I am preparing my MASC thesis for submission to the Faculty of Graduate Studies at Dalhousie University, Halifax, Nova Scotia, Canada. I am seeking your permission to include a manuscript version of the following paper(s) as a chapter in the thesis:

Manufactured aggregate from cement kiln dust
Craig Lake, Hun Choi, Colin D. Hills, Peter Gunning, & Idris Manaqibwala
Ahead of Print, pp. 1-12
Published online: December 12, 2016
http://doi.org/10.1680/jenge.15.00074

Canadian graduate theses are reproduced by the Library and Archives of Canada (formerly National Library of Canada) through a non-exclusive, world-wide license to reproduce, loan, distribute, or sell theses. I am also seeking your permission for the material described above to be reproduced and distributed by the LAC (NLC). Further details about the LAC (NLC) thesis program are available on the LAC (NLC) website (www.nlc-bnc.ca).

Full publication details and a copy of this permission letter will be included in the thesis.

Yours sincerely,

Hun Choi

Permission is granted for:

a) the inclusion of the material described above in your thesis.

b) for the material described above to be included in the copy of your thesis that is sent to the Library and Archives of Canada (formerly National Library of Canada) for reproduction and distribution.

Name: _____ Title: _____

Signature: _____ Date: _____